

Posters Session A

Monday, September 5

PA1

IN SITU PIEZOELECTRIC STUDIES OF PZT THIN FILMS BY X-RAY MICRODIFFRACTION

T.W. Cornelius¹, C. Mocuta², S. Escoubas¹, E. C. Lima³, E. B. Araújo⁴, O. Thomas¹¹Aix Marseille Université, CNRS, Université de Toulon, IM2NP UMR 7334, 13397 Marseille, France²Synchrotron SOLEIL, Gif-sur-Yvette, France³Universidade Federal do Tocantins, Porto Nacional, TO, Brazil⁴Departamento de Física e Química, Universidade Estadual Paulista, Ilha Solteira, SP, Brazil
thomas.cornelius@im2np.fr

Within the last decade, the properties of ferroelectrics have been extensively studied. Several important devices, such as Ferroelectric Random Access Memories (FeRAMs) and Dynamic Random Access Memory (DRAM), are manufactured based on ferroelectric thin films [1, 2]. With the crescent and continuous demand for portability in consumer electronics, the understanding of the effects of miniaturization on the properties of ferroelectrics thin films becomes increasingly important. Although continuous improvements in conventional semiconductor designs are implemented, the basic physics of the size effects is, however, poorly understood. It is well known that the crystallite size plays an important role in tailoring ferroelectrics properties. For studying the piezoelectric properties of $\text{Pb}(\text{Zr}_x\text{Ti}_{1-x})\text{O}_3$ (PZT) thin films consisting of few tens of nanometer sized grains, *in situ* local probe X-ray diffraction (spot size: 10 – 50 μm) has been performed at the DiffAbs beamline at SOLEIL synchrotron [3]. For this purpose, gold electrodes were deposited on top of the thin film of which one was contacted electrically using a thin wire (see Fig. 1(a)). Constant electric fields as well as alternating ones with frequencies ranging from 60 Hz to 31 kHz were applied. The diffraction signal from an area beneath the electrically contacted electrode was monitored as a function of the applied electric field. From the shift of the position of the Bragg peak induced by the applied poten-

tial, the piezoelectrically generated strain was determined revealing “butterfly loops” [4] which are a clear signature of the piezoelectric hysteresis (see Fig. 1(b)). Measurements at different Bragg reflections demonstrate an anisotropic behavior with the largest piezoelectric coefficient along the [001] direction. Asymmetric “butterfly loops” found for thin films with a $\text{Zr}/\text{Ti} = 0.5/0.5$ composition indicate the presence of a self-polarization within the thin film (see Fig. 1(c)). These findings are supported by piezoelectric force measurements revealing an asymmetry of the hysteresis loops towards positive electric fields which evidence a macroscopic self-polarization effect in the studied PZT films.

This work was partially funded by the CAPES-COFECUB project Ph801-14.

1. J.F. Scott, C.A. Araujo, *Science* **246** (1989) 1400.
2. J.F. Scott, *Ferroelectric Memories* (Springer, Heidelberg, Germany, 2000).
3. A. Davydok, T.W. Cornelius, C. Mocuta, E.C. Lima, E.B. Araújo, O. Thomas, *Thin Solid Films* **603** (2016).
4. M.C. Ehmke, J. Glaum, M. Hoffman, J.E. Blendell, K.J. Bowman, *J. Am. Ceram. Soc.* **96** (2013) 2913.

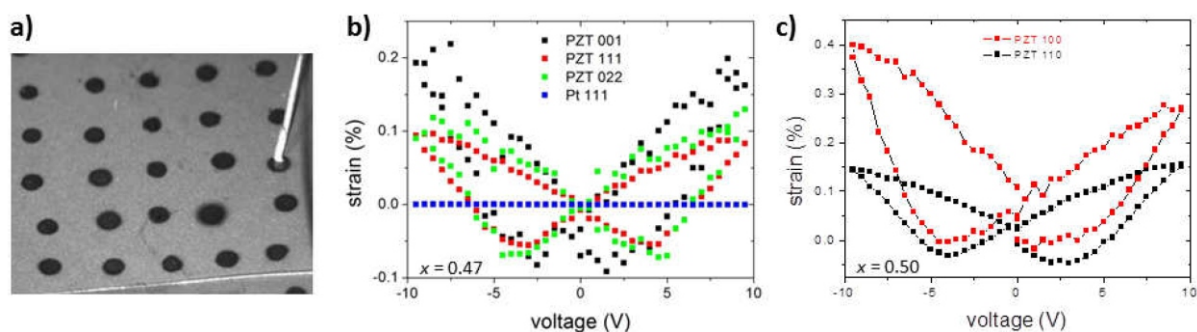


Figure 1. Piezoelectrically induced strain as a function of applied voltage for a) a $\text{Pb}(\text{Zr}_{0.47}\text{Ti}_{0.53})\text{O}_3$ and b) a $\text{Pb}(\text{Zr}_{0.5}\text{Ti}_{0.5})\text{O}_3$ thin film measured in situ by X-ray microdiffraction.



PA2

EFFECT OF INDENTATION INDUCED STRAIN ON EPITAXIAL Fe LAYERS

R. Tholapi¹, T. Slobodskyy¹, A. Zozulya², L. Liefeth¹, M. Sprung², M. Burghammer³,
M. Rosenthal³, W. Hansen¹

¹Institute of solid state physics and nanostructure, University of Hamburg, D-20355, Hamburg, Germany

²Photon Science, Deutsches Elektronen-Synchrotron (DESY), Notkestraße 85, 22607 Hamburg, Germany

³European Synchrotron Radiation Facility (ESRF), 71 Avenue des Martyrs, 38000 Grenoble, France:

rtholapi@physnet.uni-hamburg.de

Spin polarised currents have potential applications in adding complementary functions to already existing charge based CMOS technology [1]. Spin based phenomenon like spin injection, spin manipulation and spin detection are widely tested on epitaxial Fe/GaAs system. However, the efficiency of electrical spin manipulation processes at the interface is still relatively low. A modest enhancement of the spin injection efficiency due to post growth annealing of the heterojunction is related to interface state density [2] and indicates that the ferromagnet and semiconductor interface is very sensitive to external strain. For a thorough understanding of the spin transport and for fabrication of spin based devices it is essential to characterize the strain of the ferromagnetic layer at sub-micron dimensions.

In this work we study the elastic behaviour of patterned epitaxial Fe layer under external load. Recently we have integrated a commercially available Atomic Force Microscope (AFM) at P10 beamline of PETRAIII synchrotron at

DESY [3]. We used this AFM setup at ID13 beamline of ESRF as an indentation tool to apply external stress to patterned Fe layers. The AFM setup was used for both alignment and to address the sub-micron structures. We obtained rocking curves around Fe (011) reflection in Grazing Incidence Diffraction (GID) geometry at different loads using a micro-focused beam. By analysing evolution of lattice parameters during the loading process we studied the interface strain. We will also discuss the effect of ionising synchrotron radiation on sub-micron structures studied at ambient conditions.

1. S. Datta and B. Das, *Appl. Phys. Lett.* **56**, 665 (1990).
2. G. Salis, A. Fuhrer, R.R. Schlittler, L. Gross, and S.F. Alvarado, *Phys. Rev. B* **81**, 205323 (2010).
3. T. Slobodskyy, A. V. Zozulya, R. Tholapi, L. Liefeth, M. Fester, M. Sprung, and W. Hansen, *Rev. Sci. Instrum.* **86**, 065104 (2015).

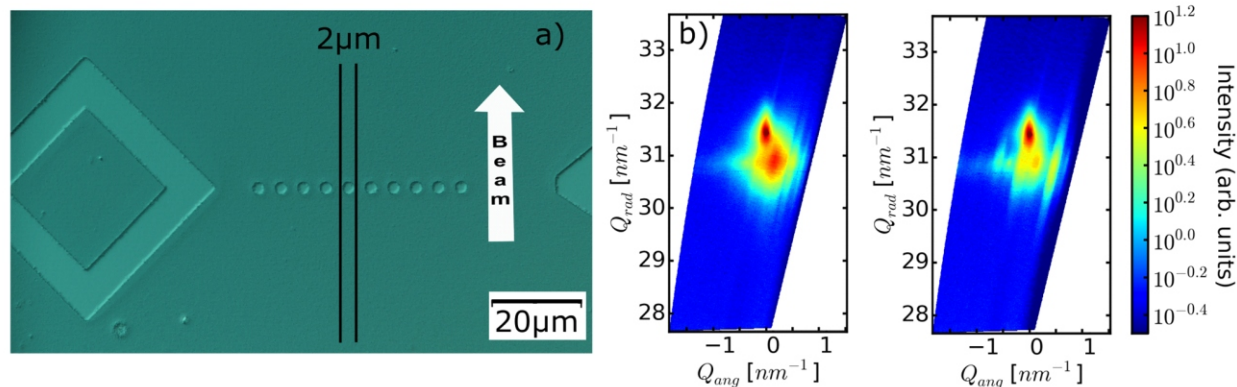


Figure 1. a) Microscopic image showing patterned Fe/GaAs structures, b) GID maps of individual structure with no load, c) with external load of 0.7 GPa.

PA3

STRUCTURE AND MORPHOLOGY OF THIN FILMS OF A BTBT DERIVATIVE: A COMBINED X-RAY REFLECTIVITY AND AFM STUDY

A. O. F. Jones,¹ H. Spreitzer,¹ B. Kaufmann,² C. Teichert,² R. Resel¹

¹Institute of Solid State Physics, Graz University of Technology, Graz, Austria

²Institut für Physik, Montanuniversität Leoben, Leoben, Austria

andrew.jones@tugraz.at

Having control over the crystal structure that molecules adopt in the solid state is an important step towards being able to maximise the efficiency of devices based on organic semiconducting materials. The inherent anisotropy of molecular systems means that it is important to orient the system correctly on a substrate and that, where polymorphism is present, the crystal structure with the most suitable properties is used. This is of particular relevance in organic thin films where a special type of polymorph, so-called surface induced or thin film phases, may appear. To better understand the parameters under which such polymorphs form, we have studied the growth of films of C₈O-BTBT-OC₈ (C₃₀H₄₀O₂S₂), a member of the high mobility BTBT family of organic semiconductors. Films have been produced by

vapour deposition, ranging in thickness from a sub-monolayer to thick, multiplayer films. Grazing incidence X-ray diffraction and X-ray reflectivity (XRR) measurements are combined with AFM imaging to understand how different deposition parameters impact on the structure and morphology of the films. It is found that a pronounced layer-by-layer growth occurs and that the previously observed surface-induced structure always forms regardless of changes to the deposition parameters showing the enhanced stability of this phase in thin films. The XRR fitting worked particularly well for very thin layers where electron density profiles could be generated showing the different parts of the molecule (e.g. alkyl chain, conjugated core) and how they are arranged within the film.

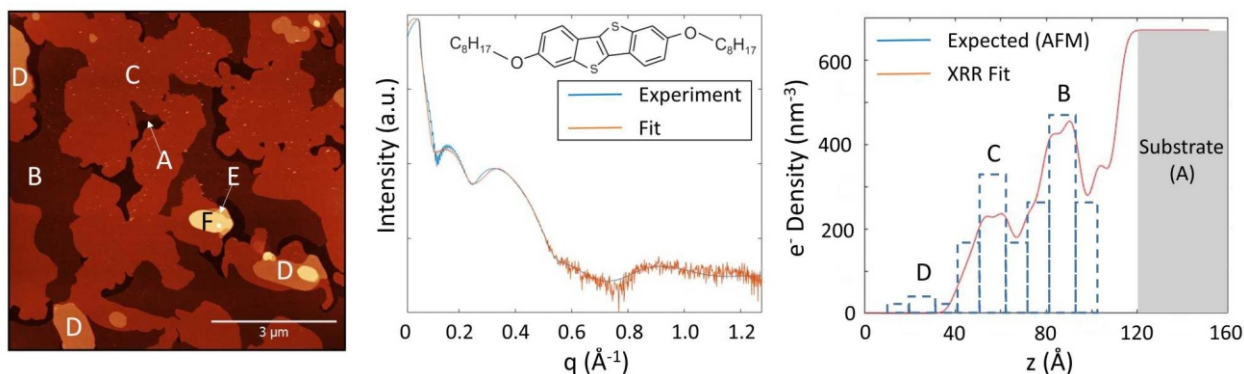


Figure 1. An AFM image of a 5 nm thick C₈O-BTBT-OC₈ film showing different layers within the film (left), the X-ray reflectivity curve and model fit for the same film with the molecular structure shown in the inset (centre), and the electron density profile of the film generated from the XRR model fit and compared with the expected values determined from the layer coverage in the AFM measurements (right).



PA4

STRUCTURAL PROPERTIES OF PICENE-PERFLUOROPENTACENE AND PICENE-PENTACENE BLENDS: SUPERLATTICE FORMATION VERSUS LIMITED INTERMIXING

J. Dieterle¹, K. Broch^{1,2}, A. Hinderhofer¹, H. Frank¹, J. Novak³, A. Gerlach¹, T. Breuer⁴, R. Banerjee^{1,5}, G. Witte⁴, and F. Schreiber¹

¹Institut für Angewandte Physik, Universität Tübingen, Germany

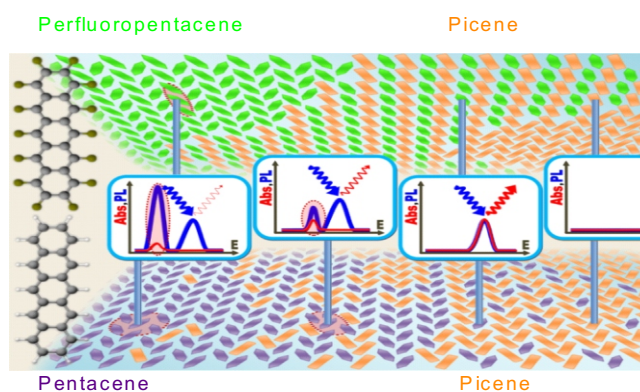
²Cavendish Laboratory, University Cambridge, UK

³Central European Institute of Technology, Masaryk University, Czech Republic

⁴Fachbereich Physik, Universität Marburg, Germany

⁵Department of Physics, Indian Institute of Technology, Gandhinagar, India

The structure and morphology of mixed thin films of picene ($C_{22}H_{14}$, PIC) and perfluoropentacene ($C_{22}F_{14}$, PFP) as well as mixed thin films of PIC and pentacene ($C_{22}H_{14}$, PEN) grown by simultaneous co-evaporation is investigated using X-ray diffraction, atomic force microscopy, and near-edge X-ray absorption spectroscopy. For both systems we find mixing on the molecular level and the formation of mixed structures. However, due to the strongly different interactions in both mixtures the ordering is fundamentally different. For the equimolar PFP:PIC mixtures, we observe the formation of two different mixed polymorphs with unit cells containing 2 PIC and 2 PFP molecules depending on the growth temperature. One of these polymorphs is a superlattice with in-plane compound segregation. The other polymorph is less symmetric and results only in a very short ranged in-plane ordering. In contrast, the PEN:PIC mixtures form crystals with unit cell parameters continuously changing with the molar concentrations between those of the pure compounds. The position of molecular species within the crystal lattice is statistical. Surprisingly, for higher concentrations of PIC we observe phase separation of surplus PIC



molecules which corresponds to a limited intermixing of the two compounds. Finally, the results are discussed in the context of other organic semiconductor binary mixtures showing that besides chemical composition and steric compatibility the intramolecular arrangement of the atoms important for intermolecular interactions significantly influences the structure formation in organic semiconductor blends.

PA5

IN-SITU X-RAY DIFFRACTION ANNEALING STUDY ON AN ANTHRADITHIOPHENE DERIVATIVE

J. Rozbořil^{1,2}, K. Broch³, O. Bubnova³, Chaw-Keong Yang³, H. Sirringhaus³, J. Novák^{1,2}

¹CEITEC, Masaryk University, Kamenice 5, 62500 Brno, Czech Republic

²Department of Condensed Matter Physics, Faculty of Science, Masaryk University, Kotlářská 2, 61137 Brno, Czech Republic

³Department of Physics, Cavendish Laboratory, JJ Thomson Avenue, Cambridge, CB3 0HE, UK
jj.rozboril@gmail.com, novak@physics.muni.cz

Organic semiconductors have been intensively studied in the last two decades because of their great application potential for fabrication and development of electronic and optoelectronic devices such as organic solar cells and organic field-effect transistors. Electronic properties of organic semiconductors such as charge-carrier mobility are strongly dependent *inter alia* on the molecular order, which is influenced by deposition method, substrate material, and processing conditions. One of the promising materials in

this field is 5,11-bis(triethyl silylethynyl) anthradithiophene (TES-ADT), which is solution-processable and demonstrates high charge-carrier mobility [1].

In this work we investigate post-growth thermal annealing induced structural changes of drop casted TES-ADT thin films on Si substrates prepared at different conditions. We measured *in situ* specular X-ray reflectivity (see Fig. 1) and grazing incidence X-ray diffractometry.

ction at sample temperatures from RT up to 160 °C using a laboratory diffractometer equipped with a rotating anode X-ray source. Besides of phase transitions already reported in Ref. [2], we report on continues thermally induced changes of TES-ADT lattice parameters. The thermal expansion coefficients and changes of the elementary cell angles are much distinct for the respective phases of the organic semiconductor.

1. M. M. Payne, S. R. Parkin, J. E. Anthony, C. C. Kuo, T. N. Jackson, *J. Am. Chem. Soc.*, **127**, (2005), 4986.
2. L. Yu, X. Li, E. Pavlica, F. P. V. Koch, G. Portale, I. da Silva, M. A. Loth, J. E. Anthony, P. Smith, G. Bratina, B. Ch. Kjellander, C. W. M. Bastiaansen, D. J. Broer, G. H. Gelinck, N. Stingelin, *Chem. Mater.*, **25** (9), (2013), 1823-1828.

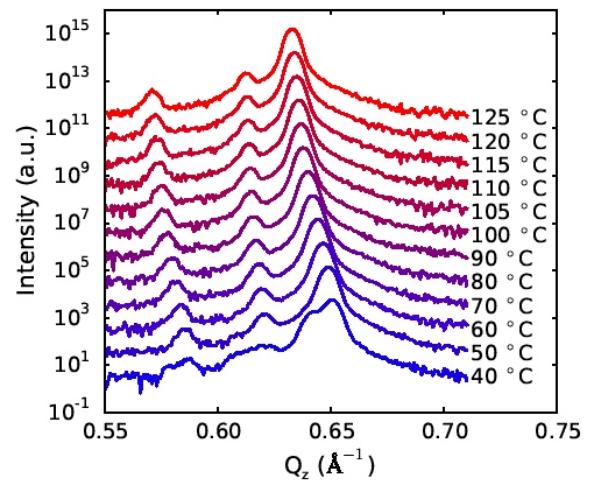


Figure 1. Specular scans measured during cooling of TES-ADT thin film in the phase.

PA6

X-RAY ANALYSIS OF STRAINED EPITAXIAL LAYERS IN SKEW GEOMETRY

P. Zaumseil

IHP, Im Technologiepark 25, Frankfurt (Oder), Germany
 zaumseil@ihp-microelectronics.com

To analyse composition and strain in epitaxial layer systems like $\text{Si}_{1-x}\text{Ge}_x$ on Si, $\text{Ge}_{1-x}\text{Sn}_x$ on Ge, or compound layers it is necessary to determine both off-plane (a_1) and in-plane lattice (a_0) parameter. This is typically done by reciprocal space mapping using asymmetric reflections or a combination of specular (a_1) and in-plane (a_0) measurements. In [1] we introduced the so-called \cos^2 method that uses reflections in skew geometry, where the sample is tilted by an angle around an axis parallel to the beam direction for $2\theta = 0^\circ$, to determine a_0 with high precision without a direct in-plane measurement.

But for strained layers the tilt angle of inclined lattice planes relative to the surface is different for sub-strate and layer, which results in completely different χ - 2θ diffraction curves depending on the selected χ value in skew ge-

ometry. In this presentation we want to analyse in detail the relation between diffraction curves of strained layer systems and χ values in skew geometry and discuss possible applications.

To analyse the χ - 2θ relation for skew reflections with high resolution, it is necessary to realise low angular divergence not only in the diffraction plane but also perpendicular to it. A SmartLab μHR from Rigaku was used, which generates due to its confocal Max-Flux optics a beam divergence of about 0.04° in both planes that was further reduced in the diffraction plane by a Ge(400)x2 crystal collimator. Figure 1a shows the intensity vs. χ for the (202) diffraction in skew geometry at the 2θ position of the Si substrate and the SiGe peak for a $\text{Si}_{0.8}\text{Ge}_{0.2}/\text{Si}$ sample. The obtained χ peak distance of 0.374° is in good agreement

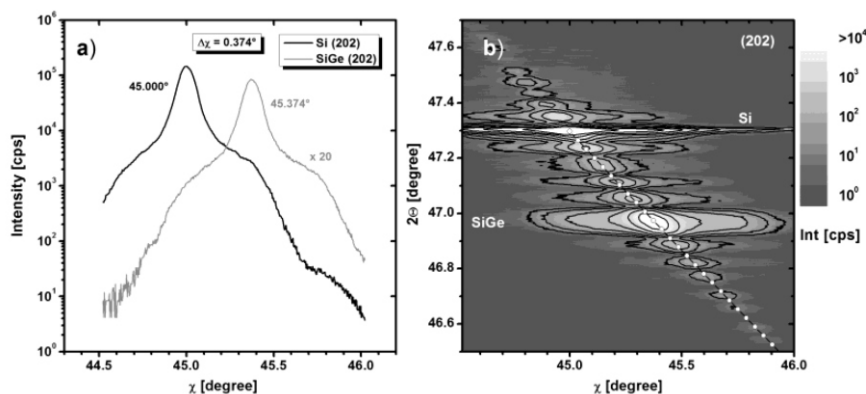


Figure 1. (a) Intensity vs. χ for the (202) diffraction in skew geometry (pseudomorphic sample) at the 2θ position of the Si substrate and the SiGe peak; (b) χ - 2θ intensity map of the (202) diffraction of the same sample.



with the theoretical value of 0.375° . The 2θ - intensity map in figure 2b shows that the measured intensity distribution follows a straight line. The line with dot symbols starting from the Si substrate peak indicates the calculated peak positions for pseudomorphic SiGe layers with increasing Ge content.

Using the intensity as a function of 2θ taken along the straight line in figure 1b, it is now possible to perform a

curve simulation. Obtained values for layer thickness are in good agreement to simulations of specular (004) curves.

This technique offers additional freedom in the selection of diffraction netplanes. It was successfully used for different samples including superlattice structures and relaxed SiGe layers on Si substrate.

1. P. Zaumseil, *J. Phys.D: Appl. Phys.*, **41**, (2008), 135308.

PA7

IN-SITU X-RAY ANALYSIS OF NICKEL SILICIDE FORMATION

P. Zaumseil, D. Wolansky

IHP, Im Technologiepark 25, Frankfurt (Oder), Germany
zaumseil@ihp-microelectronics.com

Metal silicides are applied as low-resistance contact materials in microelectronics technology. Progressive down scaling of transistor dimensions implies the need for further decreasing of silicide layer thickness and following the search for materials of lowest resistivity. Ni silicide is the candidate of choice, even its phase diagram is rather complex. Its main phases and transformation temperatures starting from a pure Ni layer on Si substrate are: Ni₂Si (250 °C), NiSi (350 °C), and NiSi₂ (800 °C). But only NiSi shows the desired low resistivity (10.5 – 15 $\mu\Omega\text{cm}$). Process optimisation requires complex knowledge about the thermal behaviour in the Ni diffusion processes including activation energies for the phase transformations.

Here we want to measure the activation energy for Ni₂Si and NiSi formation by isothermal in-situ XRD studies optimised concerning measuring speed and material texture on a 40 nm thick Ni layer deposited by sputtering on a 200 mm Si(001) wafer. Temperature- 2θ -intensity plots were measured with a 9kW SmartLab diffractometer from Rigaku in Bragg-Brentano (BB) geometry with Dtex-Ultra linear detector as well as in grazing incidence (2° angle of

incidence) mode (GID) with scintillation counter using a high temperature chamber DHS1100 from Anton Paar.

The Ni to Ni₂Si transition was analysed by repeated 2θ scans (2θ range: $43^\circ - 46^\circ$, 2.8 minutes per scan) at fixed temperatures (210 – 270 °C). Figure 1 shows the time dependent change of the Ni(111) and Ni₂Si(013) peak for 230 °C. The decreasing intensity of the Ni(111) peak can be fitted by an exponential function (Fig. 1b) and the time constant of this function can be used to estimate the activation energy of this process in an Arrhenius plot (Fig. 1c) as (1.55 ± 0.13) eV in good agreement with values obtained for Ni diffusion in Si.

Similar measurements were performed in GID geometry to analyse the transformation from Ni₂Si to the more randomly oriented NiSi under isothermal conditions (300 – 350 °C). An activation energy of (1.30 ± 0.15) eV was estimated for this process.

The techniques described here may be successfully used for further Ni silicide process optimisation.

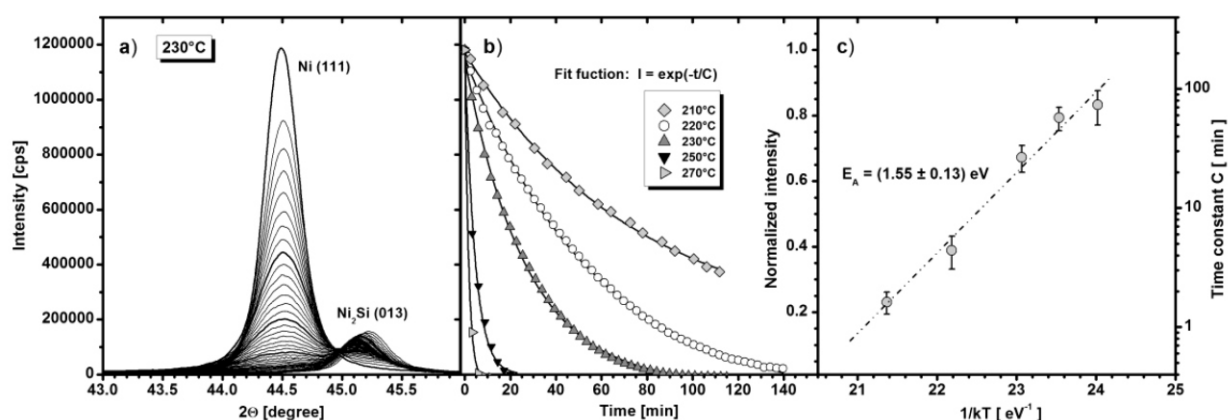


Figure 1. (a) In-situ XRD measurement (BB) of Ni to Ni₂Si transformation at 230°C, thicker lines indicate 20 minute intervals; (b) time dependent decrease of normalised Ni(111) peak height at different temperatures and fitted exponential function; (c) Arrhenius plot of time constant C to estimate the activation energy.

X-RAY ANALYSIS OF THERMAL STRAIN RELEASE IN Ge PATCHES ON Si PILLARS

P. Zaumseil¹, G. Capellini¹, A. Marzegalli², A. Cortinovis², A. Scaccabarozzi², F. Isa³,
G. Isella³, T. Schröder¹, and L. Miglio²

¹IHP, Im Technologiepark 25, Frankfurt (Oder), Germany

²L-NESS and Dept. of Materials Science, University of Milano-Bicocca, via Cozzi 55, I-20125, Milano, Italy

³L-NESS and Dept. of Physics, Politecnico di Milano, via Anzani 42, I-22100, Como, Italy
zaumseil@ihp-microelectronics.com

Ge layers of more than few nanometres in thickness grow fully relaxed on Si substrates, due to a lattice misfit of about 4.2 % between both materials. But the mismatch between the coefficients of thermal expansion gives rise to tensile strain in the Ge layer of 0.1 to 0.2 %, as soon as cooled down to room temperature, depending on the deposition or post growth annealing temperature. The corresponding stress field, especially in micrometres-thick Ge layers, causes unwanted warping or cracking. This problem of substantially reducing the thermal strain has not been satisfactorily solved, so far.

Here we present results of X-ray diffraction measurements to analyse the thermal strain release in Ge patches suspended on micrometric Si pillars, for different pillar width and patch size. These results are compared to 3D and 2D FEM simulations showing that the lateral bending of the pillar is the key aspect with increasing pillar aspect ratio.

8 nm Ge were deposited by LEPECVD [1] at 575 °C on Si(001) substrates, patterned in pillars that are arranged in square arrays, featuring different pillar periodicity, and patch size (100, 200, and 300 nm). X-ray measurements were performed with a SmartLab μ HR diffractometer from Rigaku.

Specular -2θ scans of the Ge (004) diffraction in figure 1a demonstrate decreasing strain in the Ge patches with decreasing patch size, and figures 1b,c show the tilt of the Si pillars and at the edges of the Ge patch. A more complex discussion of the strain and tilt state in these structures will be given by means of reciprocal space mappings.

1. C. Rosenblad, H. R. Deller, A. Dommann, T. Meyer, P. Schroeter, H. von Känel, *J. Vac. Sci. Technol. A*, **16**, (1998), 2785.

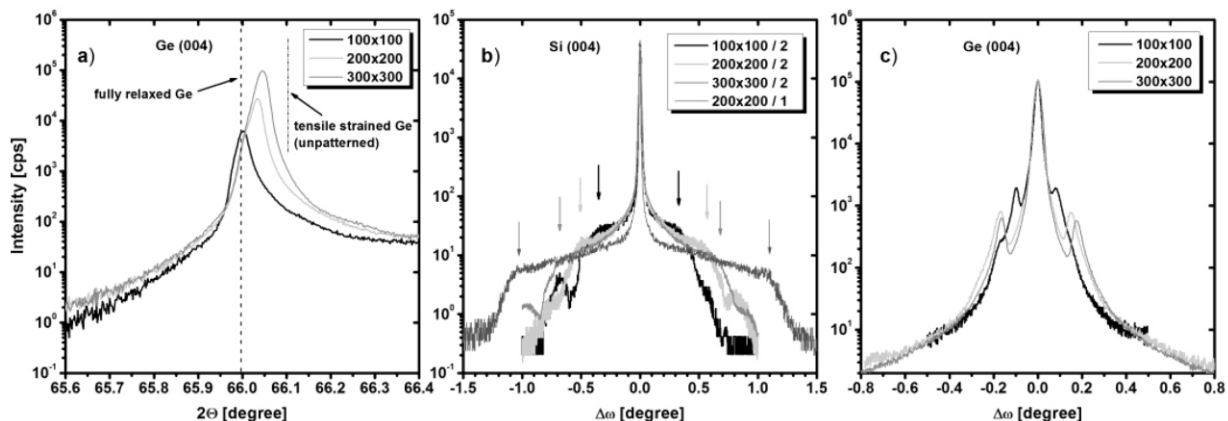


Figure 1. (a) Specular -2θ scans of Ge (004) diffraction measured on patches of different size with 2 μ m Si pillar width; (b) scans of the Si (004) substrate diffraction for patches with different size and Si pillar width; (c) scans of the Ge (004) diffraction for patches with different size and 2 μ m Si pillar width.



PA9

TIME-RESOLVED *IN-SITU* X-RAY INVESTIGATIONS DURING GROWTH OF $\text{In}_x\text{Ga}_{1-x}\text{As}$ CORE-SHELL NANOWIRE STRUCTURES

L. Feigl¹, P. Schroth^{1,2}, J. Jakob¹, S. M. M. Kashani², J. Vogel², A. Davtyan, S. Francoual, J. Strempler, U. Pietsch², and T. Baumbach³

¹*Institute for Photon Science and Synchrotron Radiation, KIT - Karlsruhe Institute of Technology, Hermann-von-Helmholtz-Platz 1, D-76344 Eggenstein-Leopoldshafen, Germany*

²*Department of Physics, University of Siegen, Emmy-Noether-Campus, Walter-Flex-Str. 3, 57072 Siegen, Germany*

³*Laboratory for Applications of Synchrotron Radiation, KIT - Karlsruhe Institute of Technology, Kaiserstr. 12 D-76131 Karlsruhe, Germany
ludwig.feigl@kit.edu*

In the framework of a current BMBF funded project we are aiming to investigate the growth of semiconductor nanowires (NWs) by means of in-situ X-ray diffraction. We make use of a portable MBE chamber [1] equipped with two Be-windows allowing for inspection of Bragg angles in a range between zero and 18 degree. Due to the compact design of the MBE chamber it can be mounted on common heavy load goniometers present at suitable synchrotron beamlines. Here we report on recent in-situ experiments performed at beamline P09 of PETRA III aiming at the nucleation, growth and elastic relaxation of an $\text{In}_{0.25}\text{Ga}_{0.75}\text{As}$ shell growing on a Ga catalysed GaAs nanowire on Si(111) substrate.

GaAs NWs were fabricated prior to the in-situ experiment and characterized by SEM to ascertain a known NW template suitable for growth of the shell. For GaAs growth a V/III ratio of $F_{\text{V/III}} = 5$ and a substrate temperature $T_S = 590^\circ\text{C}$ were used resulting in an axial growth rate of about 40 nm/min. At PETRA III the GaAs NW sample has been loaded into the pMBE again to study the InGaAs shell growth. In a first step the Ga droplet was consumed in As atmosphere to avoid continuation of axial growth. Subsequently, the shell was grown at $T_S = 470^\circ\text{C}$ and $F_{\text{V/III}} = 4$.

The 2D layer growth rate was set to 45 nm/h in order to be able to monitor the evolution of the shell by XRD.

The growth of the InGaAs shell was recorded by local reciprocal space maps around the symmetric (111) reflection and the asymmetric (311) and (220) zincblende and (10.3) wurtzite reflections. In all cases Si serves as a reference. The time resolution given by the duration of the scans is less than 3min. High resolution maps of the whole reciprocal volume were done both at growth temperature and room temperature before and after finishing growth. The gradual appearance and evolution of InGaAs Bragg reflections has been successfully observed, detailed results will be shown during the presentation.

1. T. Slobodskyy, P. Schroth, D. Grigoriev, A. A. Minkevich, D. Z. Hu, D. M. Schaadt, T. Baumbach, *Rev. Sci. Instrum.*, **83**, (2012), 105112.

We thank Thomas Keller, Andreas Stierle and David Reuther at DESY as well as Hans Gräfe, Bärbel Krause and Annette Weißhardt at KIT. The project was supported by German BMBF (05ES7CK and 05K13PS3).

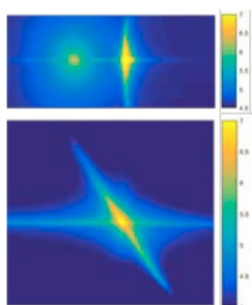


Figure 1. RSMs prior to shell growth, around Si (111) and GaAs (111) (top) and GaAs (220) (bottom).

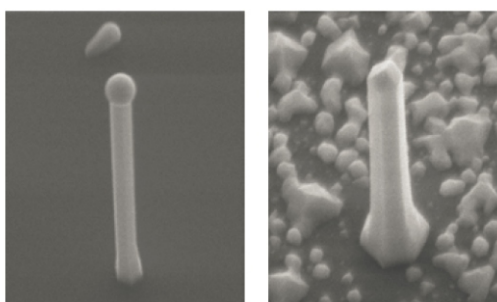


Figure 2. SEM of NW template (left) with few crystallites and SEM after InGaAs shell growth (right) with much intergrowth.

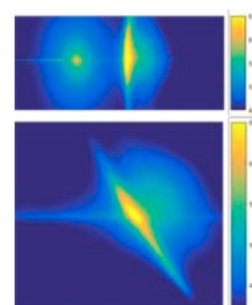


Figure 3. RSMs after deposition of shell, around Si (111) and InGaAs (111) (top) and InGaAs (220) (bottom).

IN-SITU TIME-RESOLVED XRD AND RHEED STUDY OF THE POLYTYPISM IN GaAs NANOWIRES

J. Jakob¹, P. Schroth^{1,2,3}, L. Feigl³, S. M. Mostafavi Kashani², J. Vogel², U. Pietsch², T. Baumbach^{1,3}

¹Laboratory for Application of Synchrotron Radiation, Karlsruhe Institute of Technology

²Solid State Physics, University of Siegen

³Institute for Photon Science and Synchrotron Radiation, Karlsruhe Institute of Technology
julian.jakob@kit.edu

The integration of III-V semiconductors on silicon is of particular interest to combine the standard semiconductor platform with direct band-gap materials, e.g. for on-chip optical communications [1]. One approach to overcome the lattice mismatch between both material systems is the growth of III-V nanowires onto silicon substrates.

With a portable MBE system for in-situ X-ray investigations [2], we have studied the Zincblende (ZB) – Wurtzite (WZ) polytypism in gallium arsenide nanowires [3,4]. The current setup allows for simultaneous time-resolved investigation of crystal structure evolution by means of X-ray diffraction (XRD) and by Reflecting High-Energy Electron Diffraction (RHEED) during the complete growth process.

The combination of these complementary methods provides detailed information on crystal structure and the distribution of WZ and ZB segments within the nano-structures. While XRD gives access to the shape and the crystal structure of the whole illuminated NW ensemble under inspection, RHEED as a surface sensitive technique offers the possibility to analyse the evolution of phases along the NW axis during the growth process.

In this contribution we demonstrate the feasibility of the approach at the example of the formation of crystal phases during self-catalysed growth of GaAs nanowires onto Si(111). By analysing the relative intensity of the RHEED diffraction spots as a function of growth time it is found that in case of gallium pre-deposition the probability of forming WZ is higher compared to ZB phase in the early stages of growth. In contrast, NWs grown without pre-deposition quickly tend to a low fraction of the WZ phase. The results are verified by comparison with the XRD data.

1. J. Justice, C. Bower, M. Meitl, M. B. Mooney, M. A. Gubbins, B. Corbett, *Nat Photonics*, **6**, (2012), 610-614.
2. T. Slobodskyy, P. Schroth, D. Grigoriev, A. A. Minkevich, D. Z. Hu, D. M. Schaadt, T. Baumbach, *Rev. Sci. Instrum.*, **83**, (2012), 105112.
3. M. Köhl, P. Schroth, A. A. Minkevich, J. W. Hornung, E. Dimakis, C. Somaschini, L. Geelhaar, T. Aschenbrenner, S.

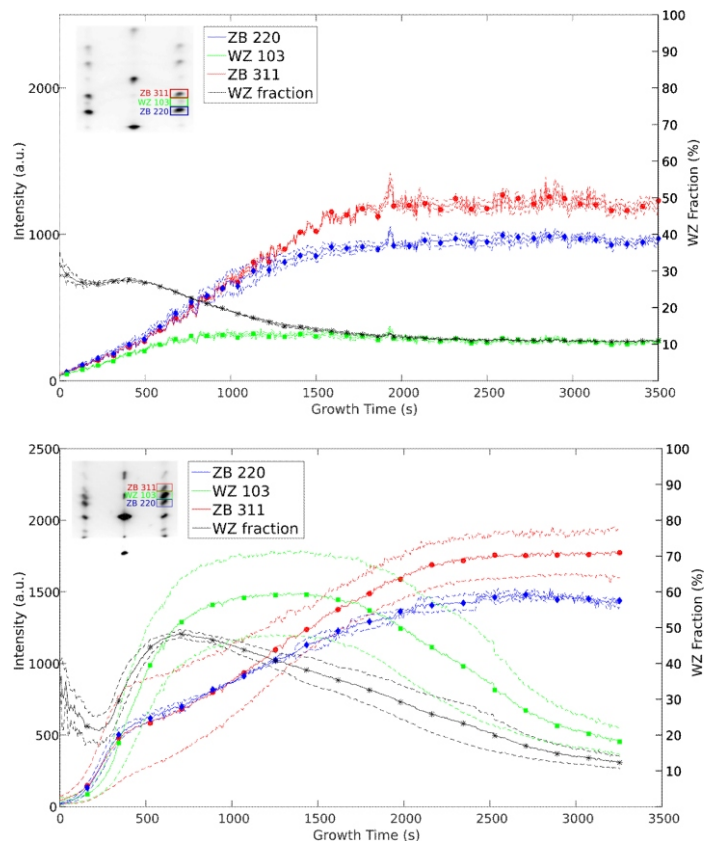


Figure 1. Time-resolved RHEED intensities of phase selective reflections of GaAs nanowires grown without gallium pre-deposition (top) and grown with gallium pre-deposition (bottom).

Lazarev, D. Grigoriev, U. Pietsch, T. Baumbach, *J. Synchrotron Rad.*, **22**, (2015), 67-75.

4. P. Schroth, M. Köhl, J. W. Hornung, E. Dimakis, C. Somaschini, L. Geelhaar, A. Biermanns, S. Bauer, S. Lazarev, U. Pietsch, T. Baumbach, *Phys. Rev. Lett.*, **114**, (2015), 055504.

We would like to acknowledge Hans Gräfe, Bärbel Krause and Svetoslav Stankov at the UHV laboratory of the Institute of Photon Science and Synchrotron Radiation, KIT and Jörg Stempffer, Sonia Francoual and David Reuther at P09, PETRA III, Desy. The work was supported by the BMBF projects (05ES7CK) and (05K13PS3).



PA11

GRAZING-INCIDENCE X-RAY CHARACTERIZATION OF SEMICONDUCTOR NANOWIRES

Mahesh Gokhale, Nilesh Kulkarni, Carina B. Maliakkal, Arnab Bhattacharya

Department of Condensed Matter Physics and Materials Science, Tata Institute of Fundamental Research, Homi Bhabha Road, Mumbai 400005, India
mahesh@tifr.res.in

Nanowires (NWs) are one-dimensional anisotropic crystalline structures having length of the order 5 to 10 μm and diameter typically less than 100 nm. These are commonly grown by the Vapour-Liquid-Solid (VLS) technique [1]. Most reports of extensive X-ray diffraction studies of NWs have been carried out typically using synchrotron radiation sources [2-10]. Very few studies carried out using laboratory XRD systems have been reported, e.g for InP [10] and GaP [11] NWs. The grazing-incidence XRD technique (GIXRD) on a laboratory XRD system can be advantageously used over standard methods to analyse NW structures. In this work we report our investigations of binary III-V (InAs, GaAs, GaP, InP) and ternary III-V (InGaP, GaAsP) nanowires grown on Si(111) substrate by VLS technique in a metalorganic chemical vapour deposition system.

GIXRD measurements were carried out for each set of NWs, and the crystal structure compared with data from standard JCPDS cards. In case of InGaP nanowires, which are in wurtzite (WZ) crystal form, change of In incorporation can be seen in the GIXRD profile (Fig. 1). The In compositions in these samples are extracted from the 2θ values. Fig. 2 shows GIXRD profile of zinc-blende (ZB) form GaAs NWs. In this case, the FWHM of the reflections from the hkl planes reduces with increasing group V/III ratio.

Crystal structure of these nanowires (WZ or ZB) depends upon the growth parameters such as temperature, V/III flux ratios etc. Details of the correlation of the crystal structure with growth parameters, determined from XRD data will be presented.

1. R. S. Wagner and W. C. Ellis, *Appl. Phys. Lett.*, **4**, 89, 1964.
2. A. L. Golovin, et al., *Acta Cryst. A*, **40**, 225, 1984.
3. H. Dosch, et al., *Phys. Rev. Lett.* **56**, 1144, 1986.
4. N. Bernhard, et al., *Z. Phys. B*, **69**:303, 1987.
5. T. Jach, et al., *Phys. Rev. B*, **39**, 5739, 1989.
6. E. A. Kondrashkina, et al., *J. Appl. Phys.*, **8**, 175 1997.
7. G. Bussone et al., *J. Appl. Cryst.*, **46**, 887, 2013.
8. J. Eymery et al., *Nano Lett.*, **7**, 2596, 2007.
9. S. O. Mariager et al, *Nanotechnol.* **21**, 115603, 2010.
10. D. Kriegner et. al. *Nanotechnology* **22**, 425704, 2011; [11] Y. Ito, *Rigaku Journal*, **25**, 1, 2009

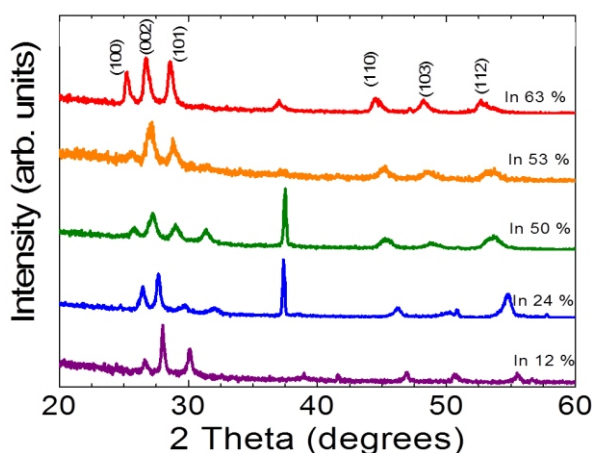


Figure 1: GIXRD scans of WZ form InGaP NWs for varying In content.

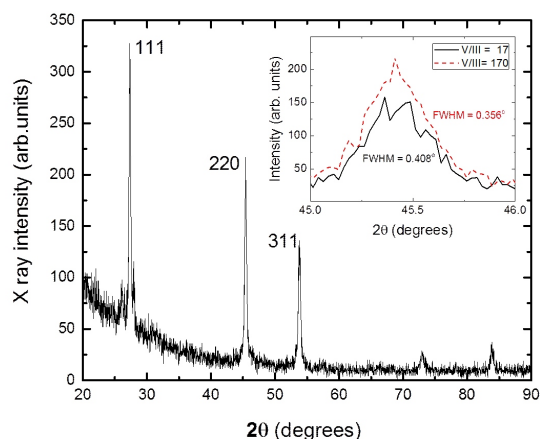


Figure 2: GIXRD scans of ZB form GaAs NWs, the inset shows an enlarged view of the (220) reflection of wires grown under different V/III ratios.

PA12

Si/GaP CORE-SHELL NANOWIRES: TOWARDS DIRECT BAND-GAP GROUP IV SEMICONDUCTORS

J. Stangl,¹ T. Etzelstorfer,¹ M. Watzinger,¹ D. Kriegner,^{1,2} H.I.T. Hauge,³ T. U. Schüllli,⁴ E. P. A. M. Bakkers³

¹Johannes Kepler University, Linz, Austria

²Charles University Prague, Czech Republic

³TU Eindhoven, The Netherlands

⁴ESRF Grenoble, France

julian.stangl@jku.at

Semiconductor nanowires exhibit a number of special properties making them interesting both for fundamental science as well as for different applications ranging from solar cells to fast transistors. In III-V semiconductors, the observation of hexagonal polytypes has spurred investigations of this crystal structure, which cannot be fabricated in bulk. Some materials show a change in band alignment from indirect to direct fundamental band gap [1], such a behaviour has also been predicted in the SiGe system. In this presentation, we will present the structural investigation of hexagonal Si material using high resolution x-ray diffraction [2]. So far, Si could not be fabricated in the hexagonal crystal structure (lonsdaleite), at least not stable under ambient conditions. Using hexagonal GaP nanowires as seed, hexagonal Si can be grown as a shell around the GaP core, and we have from this material established the bulk lattice parameters of lonsdaleite Si. The same concept is also followed for SiGe material, which is predicted to exhibit a direct band gap for high Ge concentrations.

1. S. Assali, D. Kriegner, I. Zardo, S. Plissard, M.A. Verheijen, J. Stangl, J.E.M. Haverkort, E.P.A.M. Bakkers, *Proc. SPIE* **9174**, 917405 (2014). doi: 10.1117/12.2063865.
2. H.I.T. Hauge, M.A. Verheijen, S. Conesa-Boj, T. Etzelstorfer, M. Watzinger, D. Kriegner, I. Zardo, C.

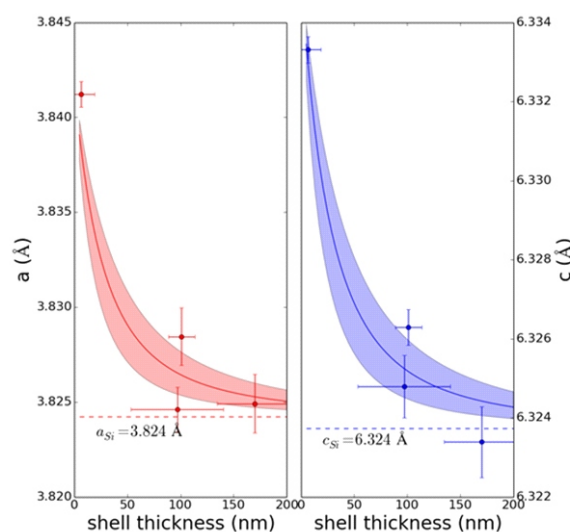


Figure 1. Average lattice parameter of hexagonal Si as a function of shell thickness in a hexagonal GaP/Si core/shell system [2]

Fasolato, F. Capitani, P. Postorino, S. Kölling, A. Li, S. Assali, J. Stangl, E.P.A.M. Bakkers, *Nano Lett.* **15**, 5855–5860 (2015). doi: 10.1021/acs.nanolett.5b01939.

PA13

THERMAL ANNEALING AND GROWTH OF A SINGLE GaAs NANOWIRE STUDIED BY IN-SITU TIME-RESOLVED X-RAY DIFFRACTION

S. M. Mostafavi Kashani¹, P. Schroth^{1,2,3}, J. Vogel¹, L. Feigl², J. Jakob², A. Davtyan¹, D. Bahrami¹, T. Baumbach^{2,3,4}, U. Pietsch¹

¹University of Siegen, Solid State Physics, Siegen, Germany

²Laboratory for Application of Synchrotron Radiation (LAS), Karlsruhe Institute of Technology (KIT), Karlsruhe, Germany

³Institute for Photon Science and Synchrotron Radiation (IPS), Karlsruhe Institute of Technology (KIT), Karlsruhe, Germany

⁴Synchrotron Facility ANKA, Karlsruhe Institute of Technology, Karlsruhe, Germany
Kashani@physik.uni-siegen.de

In the frame work of a BMBF funded project, we are running a portable MBE (pMBE) system in order to study growth processes of semiconductor nanowires (NWs) by in-situ x-ray diffraction. One of the major challenges of

this project is the in-situ study of a single NW. For this purpose, we implemented a focusing setup [1] which focuses the X-ray beam onto a pre-patterned silicon substrate with well separated NW nucleation points. Here we report on



our recent results in detecting single NWs during processing at elevated temperatures. In particular, evolution of crystal structure of a single NW was monitored at a temperature of $630 \pm 25^\circ\text{C}$ under conditions of annealing and re-growth of a single NW.

The recent experiment has been performed at the beamline P09 of PETRA III (DESY) synchrotron using a photon energy of 15keV. Prior to the synchrotron experiment, self-catalyzed GaAs NWs were grown by MBE onto Si(111) substrates covered by a $\sim 16\text{nm}$ thermal oxide layer. The substrates were patterned by Focused Ion Beam (FIB) with lateral spacing of $4\mu\text{m}$. The site-selected grown NWs had a diameter of $70 \pm 5\text{nm}$ at their bottom and an average length of $\sim 3.5\mu\text{m}$. This substrate was delivered to the pMBE chamber. Using a focused X-ray beam with a size of $4 \times 8\mu\text{m}$, we could identify signals originated from various single NWs located at the pattern. After recording reciprocal space mapping of the GaAs(111) at selected single NW positions, the substrate temperature was ramped up to a

temperature of $630 \pm 25^\circ\text{C}$. At this temperature, the 2D intensity distribution of a cut through the GaAs(111) reflection was detected with a time-resolution of ~ 2 seconds by using a Pilatus 300K detector. We thereby could record the evolution of scattering signals originating from wurtzite and zinc-blende GaAs segments [2] in a single NW during thermal annealing. Before complete thermal removal of the GaAs NWs, we opened the Arsenic and Gallium shutters with a V/III ratio of 2 and a Gallium 2D growth rate of $\sim 0.1\text{ML/s}$. The re-growth was monitored at one selected NW position and the phase composition was compared with that of the as-grown one. In the presentation, we will discuss the results in detail.

1. J. Vogel et al, Poster contribution, XTOP (2016).
2. P. Schroth, et al, *Phys. Rev. Lett.* **114** (2015).

This project has been supported by German BMBF (05ES7CK and 05K13PS3).

PA14

ANALYSE THE ELECTRON AND SPIN DENSITY PROFILES OF A MULTILAYER STRUCTURES USING WAVELET TRANSFORM ANALYSIS OF X-RAY REFLECTIVITY DATA

D. Ksenzov*, T. Sant, C. Gutt and U. Pietsch

University of Siegen, Germany
ksenzov@physik.uni-siegen.de

We present a concept to evaluate the magnetic density profiles of a tri-layer structure by means of the concept of wavelet transform of specular X-ray reflectivity pattern measured with linear polarized hard X-rays and at the Fe $L_{2,3}$ -edge using circular polarized light. Using the asymmetry profile taken from the both reflectivity data and applying the wavelet transform analysis we are able to extract the magnetic density profiles as function of the depth inside the samples. In this way, the proposed approach provides a complete picture of both the chemical and magnetic density profiles and their interface widths within the magnetic samples.

The magnetic are composed by a 10 nm ferromagnetic $\text{Ni}_{81}\text{Fe}_{19}$ (permalloy, hereafter named Py) and 10 nm of nonmagnetic (Ta) materials and capped with a 3 nm layer of Ta. The structural properties were investigated first using X-ray reflectivity curves taken in hard X-ray ranges with horizontal polarization of light in home laboratory ($E = 8.04\text{keV}$) and at the synchrotron sources DELTA ($E = 15$

keV). In addition, the soft X-ray data were taken at the EUV reflectometer of BESSY II ($E = 700\text{-}860\text{eV}$). Both data sets were transformed into reciprocal space and used to determine the chemical (charge) density profile of the samples.

In soft X-ray range and close to a fundamental absorption edge both charge and magnetic scattering contribute to the reflectivity signal. Applying circular polarized soft X-rays enables to deduce the charge magnetic interference term from the measured reflectivity profile in addition to averaged spin-profiles perpendicular to the sample surface and the overall interface roughness.

In this way, the proposed investigation provides a complete picture of the chemical and magnetic static interfacial structures of magnetic samples. Using this approach, one can study the weak changes induced by external factors (for example, the application of the external magnetic field or temperature change).

PA15

X-RAY DYNAMICAL DIFFRACTION IN NON-PERIODIC LAYERED MATERIALS WITH LARGE d -SPACING: APPLICATION TO Bi_2Te_3 - FILMS GROWN ON $\text{BaF}_2(111)$ **Sérgio L. Morelhao¹, Celso I. Fornari², Paulo H. O. Rappl², Eduardo Abramof²**¹*Institute of Physics, University of So Paulo, São Paulo, SP, Brazil*²*LAS, Instituto Nacional de Pesquisas Espaciais, São José dos Campos, SP, Brazil*
morelhao@if.usp.br

Simulations of X-ray scattering and diffraction are well-established procedures for structural analysis at nanometer and subnanometer length scales of layered materials, ranging from amorphous films to crystalline ones such as epitaxial layers on single-crystal substrates. Higher are the ordering in stacking sequences of the atomic layers, the more pronounced are the diffracted intensities at higher angles allowing more refined model structures. X-ray theories are well comfortable at the limiting cases, either amorphous films or perfect periodic layer sequences, i.e. crystalline films. However, in developing new materials and processing technologies, layered materials with random layer sequences of large d -spacing can often be found. Combined with the very high dynamical range of advanced X-ray sources and instruments, this kind of material represent a challenging in theoretical approach for X-ray diffraction simulation [1].

Large d -spacing implies that diffraction peaks are relatively close to each other, compromising theoretical approaches that treat them separately. On the other hand, low order or lack of perfect periodicity produces a systematic degradation of intensity signal in diffraction peaks at higher angles. The simple kinematic approach that neglects refraction and rescattering events of diffracted photons can be good enough for weak intensity reflections and even regions in between peaks. But, strong peaks at lower angles as well as diffraction peaks from single-crystal substrates may require an approach accounting for effects of refraction and rescattering. A similar situation is found in the investigation of surface structures by scanning crystal truncation rods [2]. At the moment, refraction and rescattering effects are accounted for in dynamical diffraction theories suitable for very crystalline materials. Although long-range scans in reciprocal space, overlap-

ping of diffraction peaks, and even strain in the crystal lattice have been treated within the scope of dynamical diffraction [1-3], they are distinct approaches and potential users are discouraged by the mathematical complexity that has to be understood to adapt these approaches to each particular system under investigation. In this scenario, what would be the importance of an approach that is as simple as the kinematic one, able to account for refraction, absorption, and rescattering in any kind of layered material, and also easily implemented in computer routines for fast simulation of diffraction experiments?

In the last few years, topological insulators such as Bi_2Te_3 have attracted enormous attention due to their new properties and potential application in spintronics or quantum computing. Epitaxial films of Bi_2Te_3 with a deficit of Te in the range $0 < < 3$ have Bi:Bi bilayers (BLs) inserted in between quintuple layers (QLs) of the Bi_2Te_3 phase. The insertion of BLs during epitaxial growth does not occur uniformly, but as a statistical distribution where the grown films can be considered as a random one-dimensional Bi_xTe_y alloy rather than an ordered homologous $(\text{Bi}_2)_M(\text{Bi}_2\text{Te}_3)_N$ structure with deficit $= 3M/(M+N)$ [4, 5]. In this work, we adapt a general recursive equation [6] for simulating X-ray dynamical diffraction in layered materials, and apply it to long-range scans obtained with synchrotron radiation in a series of $\text{Bi}_2\text{Te}_{3-d}$ epitaxial films on $\text{BaF}_2(111)$ substrates, Fig. 1. Interface quality, random stacking sequences, surface finishing, and evolution of defects during growth are parameters investigated by curve fitting with the recursive equation. It demonstrates the effectiveness of this approach for describing X-ray diffraction in layered systems ranging from random to perfect periodic stacking sequences of atomic layers.

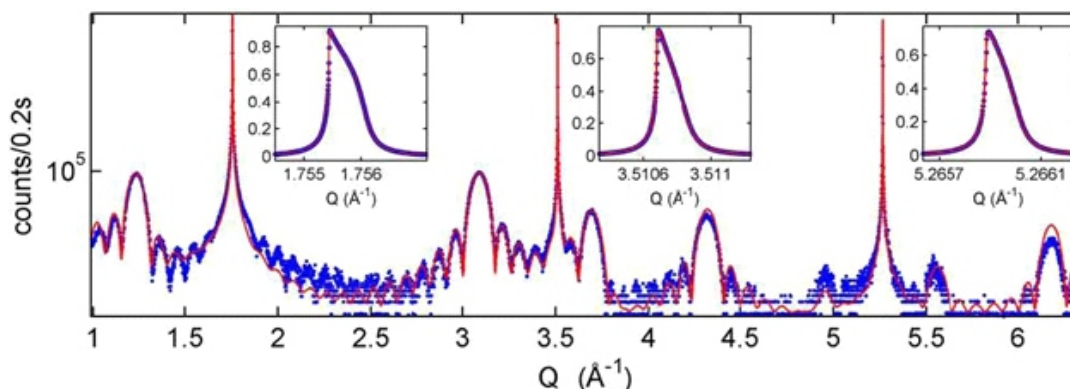


Figure 1. Long-range Q scan in $\text{Bi}_2\text{Te}_3/\text{BaF}_2(111)$. Epitaxial layers with 8 QLs. Insets: comparison of recursive equation and dynamical simulation for strong substrate reflections.



1. T. A. Alexeeva, A. I. Benediktovich, I. D. Feranchuk, T. Baumbach, A. Ulyanenkova. *Phys. Rev. B* **77**, (2008), 174114.
2. V. M. Kaganer. *Phys. Rev. B* **75**, (2007), 245425.
3. J. Gronkowski. *Physics Reports* **206**, (1991), 1.
4. H. Steiner, V. Volobuev, O. Caha, G. Bauer, G. Springholz, V. Holý. *J. Appl. Cryst.* **47**, (2014), 1889.
5. C. I. Fornari, P. H. O. Rappl, S. L. Morelhão, E. Abramof. *J. Appl. Phys.* **119**, (2016), 165303.
6. S. L. Morelhão, *Computer Simulation Tools for X-ray Analysis*. Heidelberg:Springer. 2016.

Acknowledgements are due to CNPq (Grant Nos. 142191/2014-0, 302134/2014-0, 307933/2013-0, and 306982/20129), FAPESP (Grant No. 2014/04150-0), and Brazilian Synchrotron Light Source (proposal 20150037).

PA16

X-RAY DIFFRACTION STUDY OF TOPOLOGICAL INSULATOR EPITAXIAL THIN FILMS

O. Caha¹, V. Volobuev², and G. Springholz²

¹Department of condensed matter physics, Masaryk University, Kotlářská 2, 611 37 Brno, Czechia

²Institute for Semiconductor and Solid State Physics, Johannes Kepler Universität, A-4040 Linz, Austria
caha@physics.muni.cz

Topological insulators are bulk insulators with metallic surface states exhibiting linear electronic dispersion of Dirac type. Such materials are highly attractive for spintronics [1]. The large spin-orbit interaction can provide spin polarization for novel spintronics devices [2]. The narrow gap semiconductors (Pb,Sn)Te and (Pb,Sn)Se could exhibit Rashba splitting due to its large spin-orbit interaction and the easy of doping with other heavy elements such as Bi up to several atomic percents. Its (111) surface is polar, offering surface potential that is another key ingredient for Rashba state formation. These materials have rocksalt crystallographic structure identical to a high temperature phase of ferroelectric GeTe. Changing composition of (Sn,Ge)Te ternary alloy one can tune a critical temperature of a phase transition from cubic to low-temperature rhombohedral crystalline structure. The ferroelectric phase transition changes dramatically the electric field at the sample surface. Electric field has an essential role in the surface electronic structure due to Rashba splitting.

High quality samples were grown by molecular beam epitaxy on (111) BaF₂ substrates using compound PbSe and Bi₂Te₃ sources. The crystallographic quality was studied using high-resolution X-ray diffraction. The example reciprocal space maps are shown in figure 1. The temperature dependent X-ray diffraction using liquid nitrogen cryostat was performed in the order to determine phase transition temperature.

The results of the temperature dependent X-ray diffraction are shown in figure 2. It has been found that depending of the composition phase transition temperature can be tuned up to 650 K for pure GeTe. The high temperature cubic phase undergo phase transition where cubic lattice elongates along one of equivalent {111} axis. The layer at low temperatures consist out of four different domains types corresponding to each of four {111} axis.

1. A. Manchon, et al, in: *Nature Materials* **14**, 871-882 (2015).
2. A.R. Mellnik, et al, in: *Nature* **511**, 449-451 (2014).

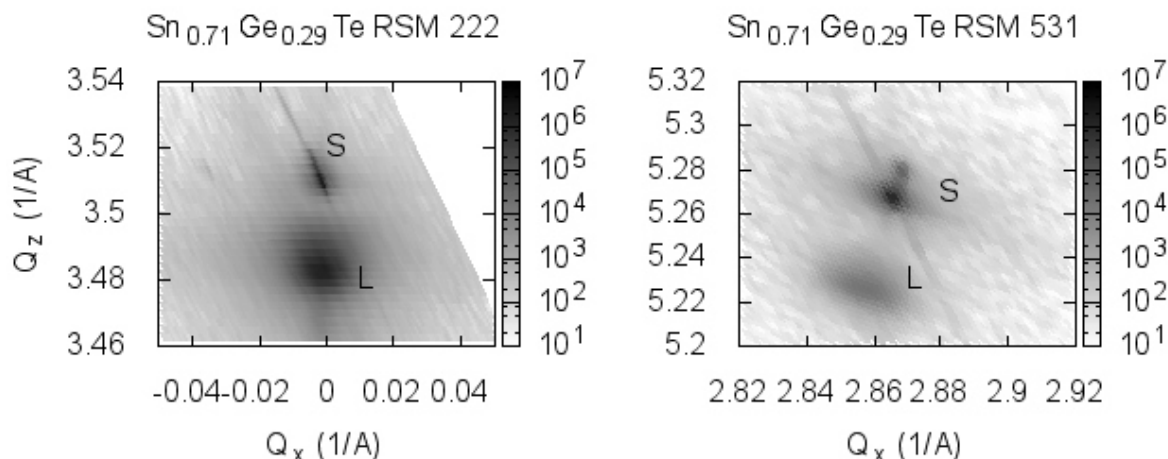


Figure 1. Reciprocal space maps measured in the vicinity of 222 and 531 reciprocal lattice points. Diffraction maxima denoted by S and L correspond to a BaF₂ substrate and (Sn,Ge)Te layer, respectively.

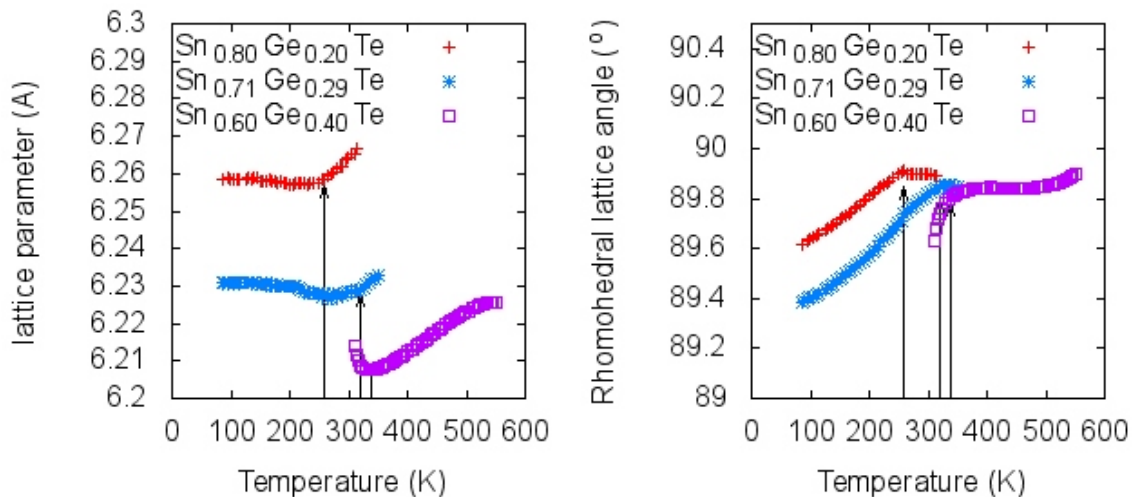


Figure 2. Temperature dependence of the lattice parameter and lattice angle of (Sn,Ge)Te layers with various composition. The arrows denote phase transition between rhombohedral and cubic lattice.

PA17

VISUALIZATION OF INHOMOGENEOUS LAYERS AND INTERFACES IN ULTRA THIN FILMS BY X-RAY REFLECTIVITY

Jinxing Jiang^{1,2}, and Kenji Sakurai^{2,1}

¹University of Tsukuba, 1-1-1, Tennodai, Tsukuba, Ibaraki, 305-0006, Japan

²National Institute for Materials Science, 1-2-2, Sengen, Tsukuba, Ibaraki, 305-0047, Japan
sakurai@yuhgiri.nims.go.jp

X-ray reflectivity technique is promising to characterize layers and interfaces in ultra thin films because of its ability to probe the atomic structures along the depth in a non-destructive manner [1]. Routine X-ray reflectivity assumes the in-plane uniformity of the sample. It is fairly important to develop spatially-resolved X-ray techniques to visualize inhomogeneous layers and interfaces. Other than XY scans of synchrotron micro beam [2], we applied image reconstruction from reflection projections [3]. In this research, we succeeded in realizing non-destructive visualization of layers and interfaces by applying synchrotron radiation. The image contrast of the technique comes from the differ-

ence of reflectivity at each point in the lateral plane of heterogeneous films. The experiment was conducted at Photon Factory, Japan. Monochromated X-rays (16keV) from a vertical wiggler insertion device are cut by several slits (See Figure 1) to form a parallel beam (vertical angular divergence: 0.02mrad), while the beam size is 0.05 (H) × 8mm (V) at sample position. The parallel beam illuminates around 8mm × 8mm sample surface at grazing incidence geometry. The reflected X-rays are recorded by a CCD camera (pixel size: 6.45 μm) as a 1D projection image. In the experiment, sample is rotated in-plane at specific interval angle until 180 degree and reflection projection is col-

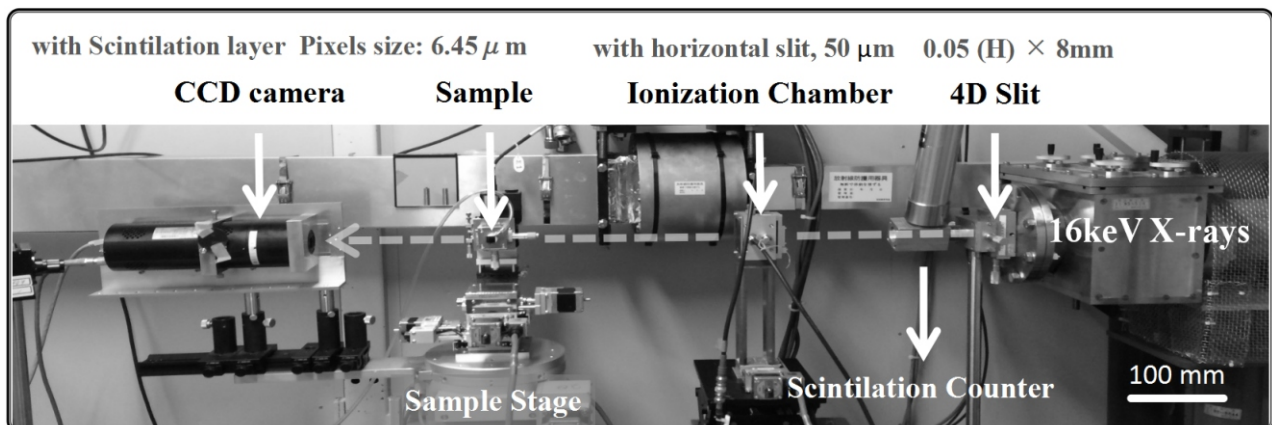


Figure 1. Side view of the instrument set at BL14B, Photon Factory (Tsukuba, Japan) to visualize inhomogeneous thin films. Synchrotron X-rays comes from right to left in the picture. Dashed arrows indicate X-rays path. Sample is vertically mounted by the pump sample holder.



lected at each interval angle. The reflection projections set is finally processed using Filtered Back-projection algorithm to reconstruct an image, which physically is a real space mapping of reflection intensities from the sample. Due to the advantage of synchrotron radiation, the incident X-rays are fairly parallel and the in-plane spatial resolution is only limited by the CCD camera pixel size. We confirmed that the in-plane spatial resolution is better than 20 nm [4], while the in-depth spatial resolution is decided by the feature of X-ray reflectivity technique (around 0.1 nm). Because of high brilliance of synchrotron radiation, the typical measuring time is shorter than 1 min.

PA18

STRUCTURE OF SELF-ORGANIZED PERIODIC SILVER DICHROMATE RINGS IN ULTRA THIN FILM

Jinxing Jiang^{1,2}, and Kenji Sakurai^{2,1}

¹University of Tsukuba, 1-1-1, Tennodai, Tsukuba, Ibaraki, 305-0006, Japan

²National Institute for Materials Science, 1-2-2, Sengen, Tsukuba, Ibaraki, 305-0047, Japan
sakurai@uhgiri.nims.go.jp

When we dispense a drop of silver nitrate solution on the top of gelatin hydrogel doped with potassium dichromate, the two inorganic chemicals produce periodic precipitate ring structures of a silver dichromate, which is known as Liesegang rings [1, 2]. This phenomenon could be found in many systems and attracts much attention because of its inherent non-linear nature and promising in micro-patterning [3-5]. Studying Liesegang pattern (LP) in ultra thin films not only helps to better understand the mechanism underlying this phenomenon, but also helps to promote appealing applications of the unique periodic structures. In addition, it may help to make the structure easier to be observed by some state of the art imaging techniques such as XRF projection - imaging [6]. So far, growing LP in ultra thin films is extremely difficult [7] because of the thin films' drying problem and fragility to the rapid capillary wetting. We successfully obtain LP in ultra thin films (see Figure 1) with the thickness down to 65 nm [8] by controlling low temperature (5 °C) and introducing equilibrium water vapor to the sample environment. X-ray reflectivity technique was applied to characterize the ultra thin films, giving not only information of thin film's thicknesses with a resolution of atomic scale, but also other useful information such as roughness, surface and interface densities. At 5 °C, gelatin hydro-gel surface shows hydrophobic nature, which helps prevent the gelatin from being rapidly wetted by capillary force. We also found new patterns existing at the out - most part of pattern in the ultra thin films which have never been reported by others to our knowledge. Fine structures of the pattern in ultra thin gelatin films were also observed by the tapping mode of atomic force microscope, which shows the rings are composed of laterally 300 – 600 nm coagulated particles.

1. K. Sakurai and A. Iida, *Jpn. J. Appl. Phys.* **31**, L113 (1992).
2. K. Sakurai, M. Mizusawa, M. Ishii, S. Kobayashi, and Y. Imai, *J. Phys.: Conf. Series* **83**, 012001(2007).
3. V. A. Innis-Samson, M. Mizusawa and K. Sakurai, *Anal. Chem.* **83**, 7600 (2012).
4. J. Jiang and K. Sakurai, Submitted to *J. Appl. Phys.*

We gratefully thank Dr. Keiichi Hirano of Photon Factory for his kind assistance during the beamtime.

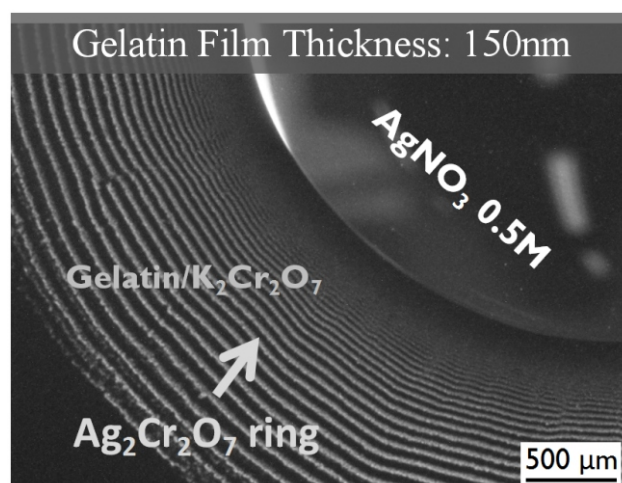


Figure 1. Optical Microscopy (OM) image of a typical periodic ring structure in ultra thin films with a thickness of 150 nm, The image were taken 4 hrs after dispensing of the silver nitrate solution droplet.

1. R. E. Liesegang, *Naturwissenschaftliche Wochenschrift*, 353–362 (1896).
2. H. K. Henisch, *Crystals in Gels and Liesegang Rings*, Cambridge University Press (1988).
3. B. A. Grzybowski, *Chemistry in Motion*, WILEY (2009).
4. R. M. Walliser etc., *Langmuir*, **31**, 1828-1834 (2015).
5. R. Klajn etc., *Nat. Mater.* **3**, 729-735 (2004).
6. K. Sakurai and M. Vysinka, In preparation for publication.
7. I. T. Bensemann, M. Fialkowski, and B.A. Grzybowski, *J. Phys. Chem. B* **109**, 2774-2778 (2005).
8. J. Jiang and K. Sakurai, Submitted to *Langmuir*.

FAST AND ACCURATE SOLUTION FOR IN-LINE MONITORING OF STRAIN FIELD THROUGH HIGH RESOLUTION X-RAY DIFFRACTION RECIPROCAL SPACE MAPPING

A. Durand^{1,2}, M. Kaufling^{1,2}, D. Le-Cunff¹, D. Rouchon² and P. Gergaud²

¹STMicroelectronics, 850 rue Jean Monnet, 38926 Crolles, France

²Univ. Grenoble Alpes, F-38000 Grenoble, France

³CEA, LETI, MINATEC Campus, F-38054 Grenoble, France
aurele.durand@st.com

As transistors continue to scale to ever smaller dimensions and in order to boost transistor performance, it has become necessary to introduce new materials such as SiGe epitaxial layer for stress engineering [1]. Consequently, to support this development, in-line strain characterization techniques are mandatory. Microscopy techniques, widely used to investigate the strain field [2], are not totally trustable due requirement of a sample preparation step and are simply not compatible with in-line process control. In a previous paper we have successfully correlated the HRXRD RSM (Reciprocal Space Maps) with the dark field electron holography microscopy technique, demonstrating the capability of HRXRD for pMOS strain field investigation [3]. However, due to the fact that the RSMs do not provide any information on the phase of the diffracted signal it is not straightforward to extract and localize the full strain field into a complex patterned structure. Still, knowing the sample geometry and the global distribution of the strain field, it is possible to extract an approaching strain field using direct analysis [4] or a phase retrieval algorithm [5]. However, both approaches require high signal to noise RSMs and are of limited interest for in-line control while measuring structures with various geometries. One way to overcome this problem is to use a reverse method. It consists in calculating RSMs from simulations of a modelled strain field. By varying the input parameters, the simulated RSM can be tuned to match to the measured one. In this paper we will illustrate this approach using a matching algorithm on a 3000 RSMs database, calculated from finite element modelling of the strain field. Fine tuning of different structures geometries and initial strain field are considered. Measured

RSMs have been selectively matched to the simulated RSMs within the database, providing strain fields as an output. This approach, easy to operate, has demonstrated to be robust, fast and precise, even on RSMs with a low signal to noise ratio. This indicates that it is a promising method for in-line strain field investigation.

1. C. Le Royer, M. Cassé, D. Cooper, F. Andrieu, O. Weber, L. Brevard, P. Perreau, J.-F. Damlencourt, S. Baudot, B. Prévitali, C. Tabone, F. Allain, P. Scheiblin, C. Rauer, C. Figuet, C. Aulnette, N. Daval, B.-Y. Nguyen, K. K. Bourdelle, J. Gyani, and M. Valenza, "Dual strained channel CMOS in FDSOI architecture: New insights on the device performance," *Solid. State. Electron.*, vol. **65–66**, pp. 9–15, Nov. 2011.
2. D. Cooper, B. Armand, J. M. Hartmann, V. Carron, and J. Rouvi, "Strain mapping for the semiconductor industry by dark-field electron holography and nanobeam electron diffraction with nm resolution," *Semicond. Sci. Technol.*, vol. **095012**, 2010.
3. A. Durand, V. Boureau, D. Lecunff, A. Hourtane, D. Benoit, A. Claverie, M. Hytch, D. Rouchon, and P. Gergaud, "Combining high-resolution X-ray reciprocal space mapping and dark-field electron holography for strain analysis in 20 nm pMOS structures," in *IEEE 15th International Conference on Nanotechnology (IEEE-NANO)*, 2015, pp. 785–788.
4. M. Medikonda, G. R. Muthinti, J. Fronheiser, V. Kamineni, M. Wormington, T. N. Adam, E. Karapetrova, A. C. Diebold, J. Valley, and T. Lane, "Measurement of periodicity and strain in arrays of single crystal silicon and pseudomorphic Si1 - xGex / Si fin structures using x-ray reciprocal space maps Measurement of periodicity and

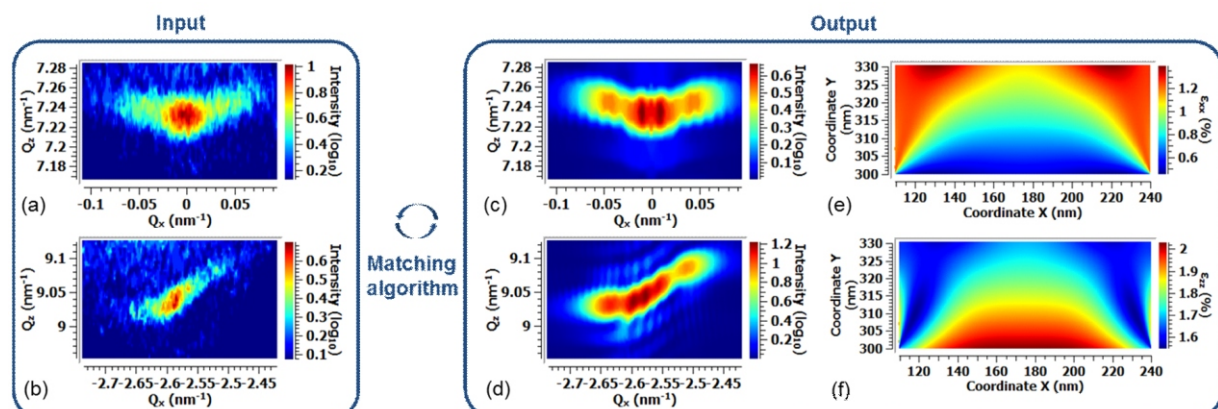


Figure 1. Measured (004) (a) and $\bar{1}\bar{1}5$, (b) RSMs, the matching simulated (004), (c) and $\bar{1}\bar{1}5$, (d) RSMs and the corresponding horizontal (e) and vertical (f) strain fields.



strain in arrays of single crystal silicon and pseudomorphic Si 1 2," *J. Vac. Sci. Technol. B Microelectron. Nanom. Struct.*, vol. **021804**, 2014.

5. A. A. Minkevich, M. Köhl, S. Escoubas, O. Thomas, and T. Baumbach, "Retrieval of the atomic displacements in

the crystal from the coherent X-ray diffraction pattern.," *J. Synchrotron Radiat.*, vol. **21**, no. Pt 4, pp. 774–83, Jul. 2014.

PA20

FROM PERIODIC TO ORDERED NON-PERIODIC NANOSTRUCTURES: GISAXS ON NANOIMPRINTED QUASICRYSTALS

M. Pflüger¹, V. Soltwisch¹, J. Xavier², J. Probst², C. Becker², M. Krumrey¹

¹Physikalisch-Technische Bundesanstalt (PTB), Abbestraße 2-12, 10587 Berlin, Germany

²Helmholtz-Zentrum Berlin (HZB), Albert-Einstein-Straße 15, 12489 Berlin, Germany
mika.pflueger@ptb.de

Nanoimprint lithography is a fast and inexpensive method for nanostructuring of large areas [1], which opens a range of applications, e.g. in solar cell manufacturing and nanofluidics. Grazing Incidence Small Angle X-ray Scattering (GISAXS) is a fast and nondestructive method for measuring large nanostructured areas, which makes it a natural fit to quantitatively assess the quality of nanoimprinted samples. The measurements were performed at PTB's four-crystal monochromator beamline at BESSY II.

We investigated arrays of nanopillars with about 0.3 μm diameter produced by nanoimprint lithography. For ordered, periodic structures, similar patterns to those produced by lamellar gratings [2] can be observed (Fig 1). Due to the statistical nature and large probed area of GISAXS, small variations arising from the production procedure can be quantified already from a single scattering pattern.

An interesting application of nanoimprint lithography is the production of large-scale two-dimensional photonic quasicrystals, which allow tuning of optical properties of surfaces [3]. Quasicrystals are ordered but non-periodic, theoretically infinite structures. Although they lack translational symmetry, their ordering results in sharp peaks in the Fourier transform as for crystals. Therefore, scattering methods show sharp diffraction peaks, making them suitable methods for the investigation of quasicrystals [4]. As in the periodic structures, a circular scattering pattern arises when the X-ray beam is aligned with the sample structure. In the q_y - q_x -map (Fig. 2), ordering and correlations in the sample plane become clearly visible.

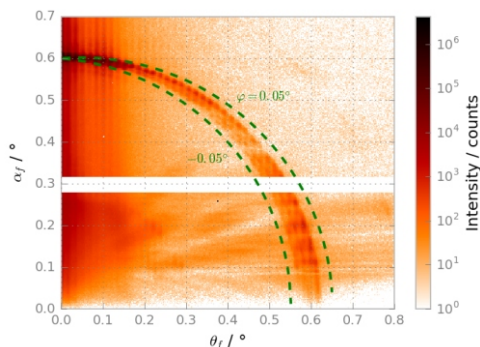


Figure 1. GISAXS pattern of a hexagonal nanopillar array, in green grating circles for a sample tilt of $\pm 0.05^\circ$.

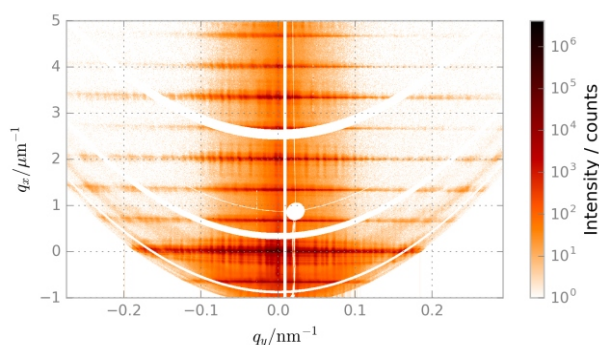


Figure 2. q_y - q_x -map of the GISAXS pattern of a surface quasicrystal with the X-ray beam aligned to a main symmetry line of the sample.

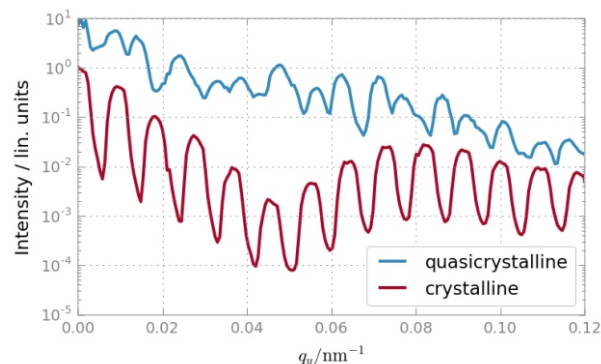


Figure 3. q_y -cut of scattering patterns of a quasicrystalline and a hexagonal sample.

We compare scattering patterns of fully periodic (i.e. crystalline) samples with those of quasicrystalline samples with a 10-fold rotational symmetry (Fig. 3), showing the richer Fourier spectrum of quasicrystals. The experimental results are compared to simulations using the Distorted Wave Born Approximation (DWBA) in order to extract further structural parameters of the samples.

1. L. J. Guo *Adv Mat* **19**, 495–513, 2007.
2. M. Yan & A. Gibaud *J Appl Cryst* **40**, 1050–55, 2007.
3. Z. V. Vardeny, A. Nahata & A. Agrawal *Nature Photon* **7**, 177–87, 2014.
4. A. Yamamoto *Acta Crystallogr Sect A* **52**, 509–60, 1996.

PA21

GRAZING INCIDENCE X-RAY SMALL ANGLE SCATTERING FOR DETERMINING SHAPE OF SEMICONDUCTOR DEVICE PATTERNS

Kazuhiko Omote, Yoshiyasu Ito

X-Ray Research Laboratory, Rigaku Corporation, Akishima, Tokyo 196-8666, Japan
omote@rigaku.co.jp

Abstract: Grazing incidence X-ray scattering is applied for evaluating fabricated periodic nano-patterned surface structure. Two-dimensional X-ray scattering patterns from the samples are collected and the shape of the sample structures are reproduced by comparing observed and calculated two-dimensional scattering intensities. The obtained results are compared with that of TEM and fairly good agreement could be achieved.

1. Introduction

The scale of semiconductor device is still continuously shrinking and line width of the device pattern will become close to ten-nanometer, soon. The wafer metrology tools have to overcome many difficult challenges in order to control the mass production processes for measuring such a small critical dimension (CD) with complex structure. For example, the electron beam size of CD-SEM is comparable with the measured CD itself, and difficult to see the bottom of narrow valley. The sensitivity of optical probes will become very low because wavelengths of the lights are much longer than the CD. In addition, uniformity of the CD, for example line width roughness (LWR), becomes more crucial for the device performances and the metrology has to have higher sensitivity for detecting such kinds of non-uniformity.

Small angle X-ray scattering (SAXS) method is one of a hopeful candidate having such capabilities for measuring CD and its uniformity. Jones *et al.* demonstrated SAXS measurements with transmission geometry [1]. Other ap-

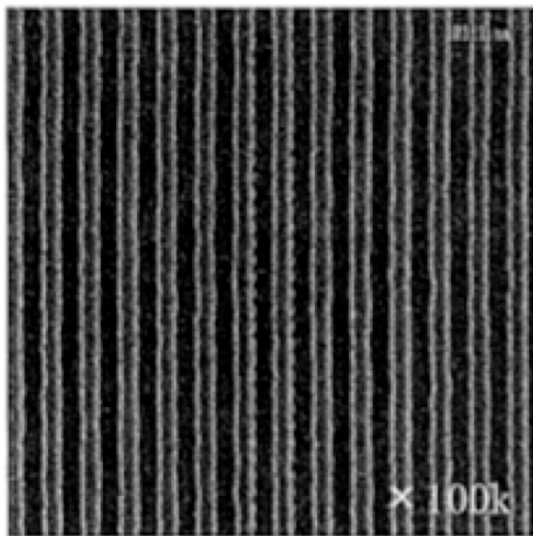


Figure 1. Scanning electron microscope image of the 100-nm pitch grating.

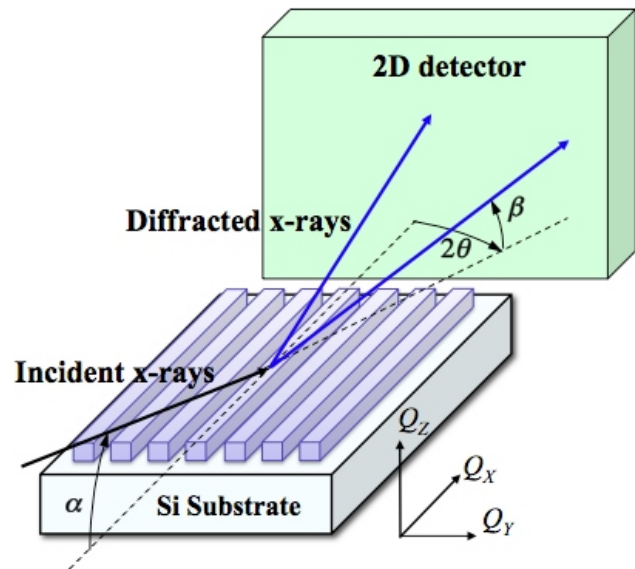


Figure 2. Experimental setup of the GIXD measurement for the surface grating. X-rays irradiate sample surface with small glancing angle and scattered x-rays having lateral scattering angle 2θ and vertical exit angle β are detected by two-dimensional detector.

proach that we developed is grazing incidence (GI) reflection geometry [2]. It is much sensitive for the surface thin structure than that of transmission geometry even the footprint of x-ray beam is much larger than that of the former. We can evaluate average structural parameters, such as width (diameter in case of dots), height, sidewall angle, rounding of edges, etc. and their fluctuations.

2. Experimental and analysis

The measured sample was periodic grating structure fabricated by electron beam lithography and dry-etching process for 70 nm thick SiO_2 layer on Si-substrate. The pitch of the grating is 100 nm as shown in Fig. 1. The measurement geometry is shown in Fig. 2. Monochromatic X-ray, with wavelength 0.15418 nm (CuK α line) is irradiated on the sample surface. The beam size at the sample position is less than 0.02 mm and 2 mm for the vertical and horizontal direction, respectively. We have selected small incident angle, $\alpha = 0.20$ degree, so as to maximize scattering intensity from the sample. Small beam-size in the vertical direction guarantees shorter footprint on the sample surface even when such small α . The scattered intensities were collected by two-dimensional detector as shown in Fig. 3 and It is directly corresponding to the structure of the patterned grating sample.

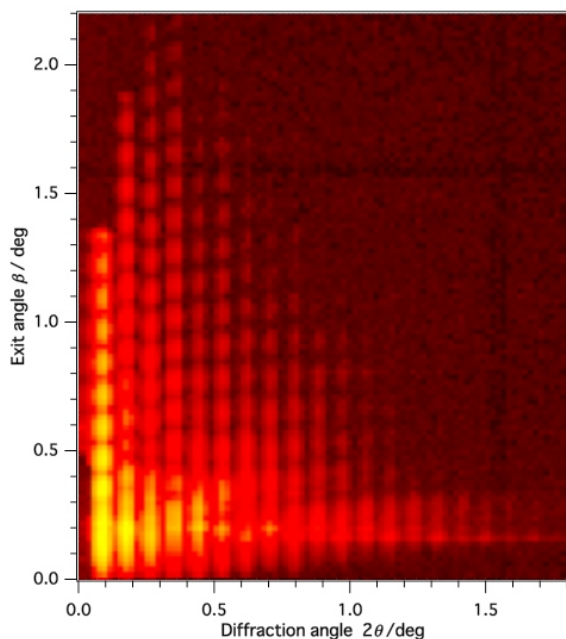


Figure 3. The observed two-dimensional diffraction pattern on the detector. Intensity is expressed by the brightness of the image. Diffraction intensity is elongated along the vertical direction and interference fringe is recognized on it.

The theoretical calculation for X-ray scattering intensity from the determined structure is well established without any arbitrary parameters within the limit of the first-order approximation. We have also considered the effects of refraction and reflection at the surface and inter-

faces using distorted wave born approximation [3, 4]. We have built an appropriate model with several critical structural parameters for the sample pattern. The introduced structural parameters are determined by using least square optimization comparing calculated and observed scattering intensity.

3. Result and discussion

The observed cross-sectional structure using optimized structural parameters is shown in Fig.4. In order to ensure the reliability of the present X-ray metrology, we have compared X-ray result with that of cross-sectional TEM. The result of X-ray (red line) is overlapped on the TEM image. We can recognize that very good agreement is obtained between them. It is very important that the present X-ray metrology is capable to figure out such precise structure in nanometer scale without destroy the sample.

4. References

1. R. L. Jones, et.al, *Appl. Phys. Lett.*, **83** (2003) 4059.
2. K.Omote, Y. Ito, Y. Okazaki, Proc. of SPIE Vol. **7638** (2010) 763811.
3. S.K. Sinha, E.B. Sirota, S. Garoff, and H.B. Stanley *Phys. Rev. B*, pp2297-2311 (1988).
4. K. Omote, Y. Ito, and S. Kawamura, *Appl. Phys. Lett.* **82**, pp544-546, (2003).

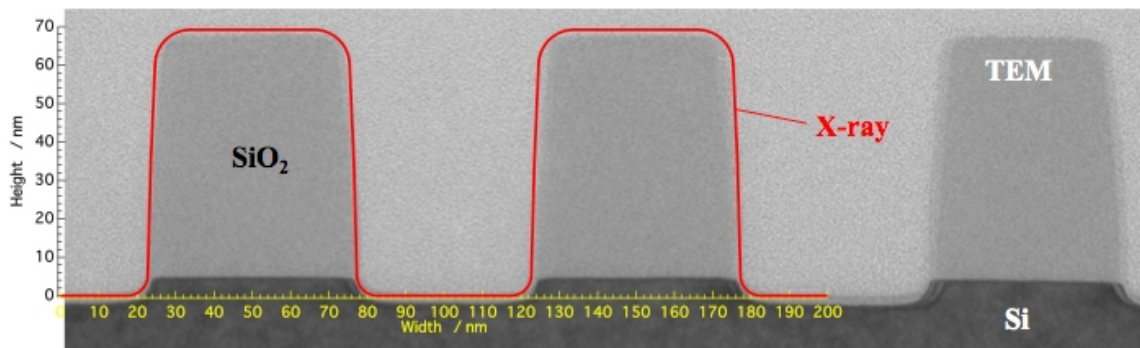


Figure 4. Comparison between the present x-ray metrology and cross-sectional TEM. The obtained profile with x-ray (expressed by red line) is overlapped on the TEM image. Very good agreement between TEM image and the present outlined profile could be achieved

PA22

CHARACTERIZATION OF SUB-NANOMETER Cr/Sc MULTILAYER SYSTEMS FOR THE WATER WINDOW

A. Haase¹, S. Bajt², P. Hönicke¹, V. Soltwisch¹ and F. Scholze¹

¹Physikalisch-Technische Bundesanstalt, Abbestr. 2-12, 10587 Berlin, Germany

²Photon Science, DESY, Notkestr. 85, 22607 Hamburg, Germany
anton.haase@ptb.de

Multilayer systems are an established method to build mirrors for short wavelength in the EUV and soft X-ray spectral range, where near-normal incidence reflectivity of single surfaces becomes negligibly small. They form artificial one-dimensional Bragg crystals designed to reflect radiation of mostly a single wavelength at a specified angle of incidence. The individual layer thickness is intrinsically connected with these two parameters to achieve constructive interference and thus high reflectivity. While systems designed for the EUV wavelength of 13.5 nm perform close to the theoretically achievable maximum reflectivity, state-of-the-art Cr/Sc mirrors for the “water window” in the spectral range between 2.2 nm and 4.4 nm wavelength yield peak reflectivities below 20% near-normal incidence. This is far behind theoretically predicted maximum values of up to 55%. The reason for this are imperfections at the interfaces of the individual layers, which are required to be chemically abrupt to achieve high optical contrast. However, due to the small wavelength very thin layer thicknesses of approx 0.7 nm are required to reflect radiation of

3.15 nm wavelength at an angle of incidence of 1.5 degrees from the surface normal.

The significant gap between the theoretically possible and actually achieved reflectivities emphasizes the need for a detailed characterization of state-of-the-art samples. We present a combined analysis based on complementary measurements of EUV and X-ray reflectivity, X-ray standing wave fluorescence (XRF) and diffuse EUV scattering. We show that an elaborate modelling of the layer system including graded interface regions is required to arrive at a consistent result describing multilayer samples with individual layer thicknesses in the sub-nanometer regime. The analysis of the data is done with a particle swarm optimizer. We verify our model based on a Markov-chain Monte Carlo sampling method. The addition of off-specular diffuse scattering measurements allows for a distinction between loss of optical contrast at the interfaces due to interdiffusion vs. roughness [1].

1. A. Haase, V. Soltwisch, C. Laubis, F. Scholze, *Appl. Optics*, **53**, (2014), 3019.

PA23

MISFIT DISLOCATION DENSITY DETERMINATION AT RELAXATION ONSET: RECIPROCAL SPACE MAP ANALYSIS OF THIN SiGe/Si LAYERS

A. Benediktovitch¹, T. Ulyanenkova², A. Mikhalychev¹, V.M. Kaganer³, M. Myronov⁴,
A. Ulyanenkov⁵

¹Atomicus OOO, Minsk, Belarus

²Rigaku SE, Ettlingen, Germany

³Paul-Drude Institut für Festkörperelektronik, Berlin, Germany

⁴Warwick University, Coventry, UK

⁵Atomicus GmbH, Karlsruhe, Germany

andrei.benediktovitch@atomicus.by

The growth of high quality Ge layers directly on Si substrate has a broad range of potential applications as a channel material in the high-mobility metal-oxide-semiconductor field-effect-transistors (MOSFET). However, due to 4.2 % mismatch between Ge and Si, the growth of high quality layer is hindered by a strain relaxation resulting in a formation of misfit dislocation network on layer-substrate interface. The monitoring of the defect state of thin epitaxial films can be performed by using a number of techniques, including the high resolution x-ray diffraction, which is one of the most advantageous one due to non-destructive character.

The appearance of the x-ray diffraction reciprocal space maps (RSM) measured from above described structures is conditioned by the dislocation induced displacement fields and is well known for both limiting cases: in the case of dislocation-free thin epitaxial layers the scattered x-ray intensity on RSM is determined by coherent scattering resulting in narrow delta-function like strips, whereas in the case of thick relaxed layers the diffuse scattering from misfit dislocations is observed, which results in broad symmetric ellipse-like peaks [1, 2]. During the lattice relaxation process, an intermediate situation is observed when both coherent and diffuse signals are present.

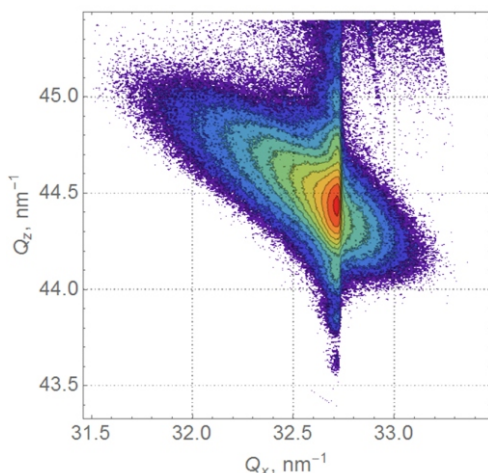


Figure 1. An example of RSM from $\text{Si}_{0.4}\text{Ge}_{0.6}$ 29 nm layer on Si(001), reflection (224).

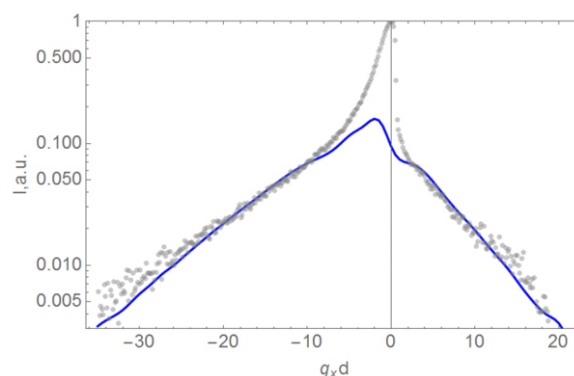


Figure 2. An RSM from Fig.1 integrated over q_z direction together with calculated diffuse contribution.

In the present work, we analyze the crossover between the two regimes described above with a special focus on diffuse scattering in the presence of coherent signal. In this regime, it comes out that diffuse intensity slope in the $-q_x$ direction follows an exponential behavior, in contrast to the Gaussian shape in the case of large dislocation density [2]. In the case of asymmetric reflection, the peak comes out to be essentially asymmetric. The developed analysis was applied to process the RSMs from $\text{Si}_{0.4}\text{Ge}_{0.6}/\text{Si}(001)$ structures that supported the drawn conclusions, Figs 1,2.

1. A. Benediktovitch, I. Feranchuk and A.Ulyanenko, *Theoretical Concepts of X-ray Nanoscale Analysis*, Springer, 2014.
2. V.M. Kaganer, R. Köhler, M. Schmidbauer, R. Opitz and B. Jenichen *Phys. Rev. B*, **55**, (1997), 1793.

PA24

THE MICROSTRUCTURE OF SI SURFACE LAYERS AFTER He^+ PLASMA IMMERSION ION IMPLANTATION AND SUBSEQUENT ANNEALING

A. Lomov¹, K. Shcherbachev², Y. Chesnokov³

¹*Institute of Physics and Technology Russian Acad. of Sciences, Moscow, Russia*

²*National University of Science and Technology MISiS, Moscow, Russia*

³*National Research Centre "Kurchatov Institute", Moscow, Russia
chsterb@mail.ru*

The progress in Si CMOS technology is connected with creation of advanced properties of substrate subsurface layers. They can be realized by a high-dose He^+ ion implantation into a silicon wafer. During this process the complex multilayer structure consisting of amorphous, helium-filled bubbles, voids and a damaged crystal layer is formed. Plasma-immersion ion implantation (PIII) is one of the coming techniques to form such a structure at a nanometer scale. A variety of phase states of material of a silicon wafer demands to involve complementary methods. This report is devoted to the study of evolution of a microstructure of Si surface layers after high-dose low-energy He^+ PIII and subsequent annealing by X-ray reflectivity (XRR), a

high-resolution X-ray diffraction (HRXRD) and a transmission electron microscopy (TEM).

Samples 30×40 mm in size were cleaved out from p-type ($\rho = 12 \text{ cm}$) Cz-Si(001) wafer. The high-dose ($D = 5 \times 10^{17} \text{ cm}^{-2}$) low-energy ($E = 2 \text{ keV}$) implantation of He^+ ions was performed at room temperature in a plasma-immersion low-voltage ion implanter, equipped with an inductively coupled plasma source. The target temperature during the process did not exceed $100 \text{ }^\circ\text{C}$. After implantation the samples were annealed in vacuum at 580 and $800 \text{ }^\circ\text{C}$ for 30 min.

The structural changes in the surface layer of the samples after implantation and the subsequent annealing were

studied in a triple-axis geometry in a vicinity of Si(004) reflection by using a multipurpose SmartLab (Rigaku Corp., Japan) diffractometer equipped by 9kW copper rotating anode. To get more detailed information about a local structure of the damaged layer and He-bubbles, the samples were investigated by TITAN 80-300 transmission scanning electron microscope (FEI, USA).

On the base of RSM data, the intensity distribution of coherent scattering was used for determination of strain and Debye – Waller factor depth profiles. The profiles showed a formation of three regions in the damaged layer: (i) amorphous layer on the surface, (ii) the tensile strained layer located at the depth corresponding to ion projected

length R_p (~ 25 nm), and (iii) the tensile strained layer located at the depth $\sim 2R_p$, corresponding to radiation-induced interstitial-type defects forming clusters (rod-like defects and dislocation loops) in the annealed samples. Comparison of XRR and HRXRD results showed that the helium-filled bubbles located in a low-density sublayer at the depth of about R_p is a major source of the tensile strain in the damaged layer. These bubbles are a source of well pronounced off-specular scattering that can be characterized by a high-resolution XRR. TEM images confirmed the existence of the multilayer structure of the damaged layer. The characteristic bubble size is estimated to be 5–20 nm.

PA25

IN-SITU GISAXS INVESTIGATION OF THERMAL AND SOLVENT ANNEALING OF HIGH-BLOCK COPOLYMERS

J. Garnier^{1,2}, J. Arias-Zapata^{1,2}, O. Marconot^{1,4}, S. Arnaud^{1,3}, S. Böhme^{1,2},
C. Girardot^{1,2}, D. Buttard^{1,4}, M. Zelsmann^{1,2}

¹Universit  Grenoble Alpes, F-38000 Grenoble, France

²CNRS, LTM, F-38000 Grenoble, France

³CEA, LETI, MINATEC Campus, F-38054 Grenoble, France

⁴CEA, INAC-PHELIQS, F-38000 Grenoble, France
denis.buttard@cea.fr

Directed Self-Assembly (DSA) of Block CoPolymers (BCPs) is an effective approach to produce thin films with various nano-sized patterns. As a consequence, DSA was introduced in the International Technology Roadmap for Semiconductors (ITRS) as a potential solution in order to complement advanced optical lithography techniques by enhancing its resolution. Due to its ease of processing, a large majority of the lithographic BCP work reported so far concerned polystyrene-block-polymethylmethacrylate (PS-b-PMMA). Nevertheless, its Flory-Huggins parameter (measuring the incompatibility between the two blocks) is not very high ($\chi = 0.06$ at 25 °C), limiting the resolution to about 15 nm. Researchers show now increased attention to BCPs with a higher Flory-Huggins parameter due to their improved resolution (possibility to fabricate sub-8 nm features). Among those, polydimethylsiloxane (PDMS) containing materials (polystyrene-block-polydimethyl-

siloxane (PS-b-PDMS) and Poly(D,L-lactic acid-b-dimethylsiloxane-b-D,L-lactic acid) (PLA-b-PDMS-b-PLA)) are particularly attractive. Their Flory-Huggins interaction parameter is relatively large and the PDMS block can readily form silicon oxide structures under an oxygen plasma whereas the PS block is degraded under the same treatment. This is leading to a SiO₂-like nanolithography mask that is well suited for pattern transfer in underlayers by plasma etching [1]. However, due to the high interaction parameter of this polymer, thermal diffusion is limited (i.e. the self-assembly process is extremely long) and non-standard processes have to be used. The most typical one is the so-called solvent annealing (SVA) process [2] where the sample is swelled by exposing it to solvent vapors, overcoming the diffusive energy barrier and allowing the self-assembly step to proceed at room-temperature. Nevertheless, to be easily introduced in a microelectronics

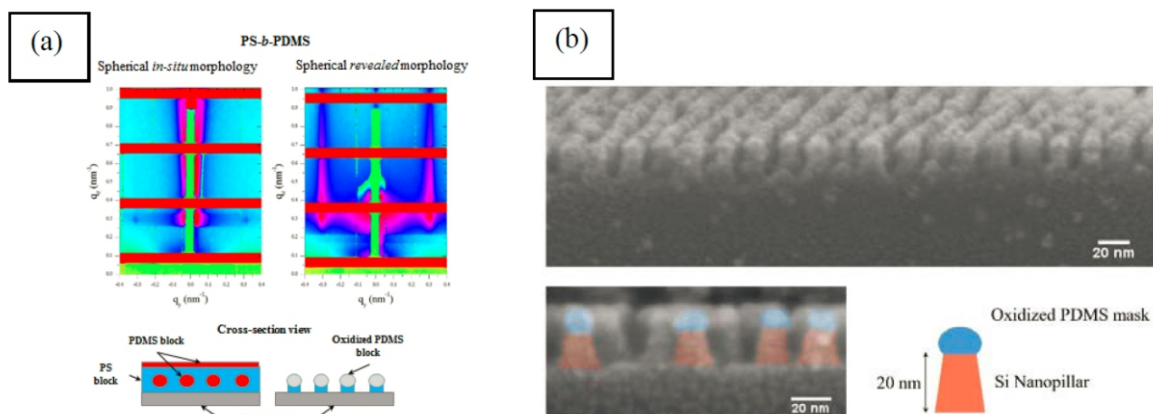


Figure 1. Ex-situ GISAXS measurements of PDMS spheres a) at two different steps of the etching process (before and after the spheres revelation), b) Cross-section SEM images of direct Si transfer of sub-10 nm PDMS spheres by RIE plasma



fab, SVA and or harmful solvents generally associated with this treatment should be avoided if possible. This is the reason why thermal annealing alone should also be investigated on these materials. Then, to allow self-organization to take place in few minutes, dedicated BCP formulations presenting higher mobility (by including homopolymers, plasticizers or salts) are considered.

During these experiments, we first measured ex-situ samples (organized before experiments) with different periodicities (from 18 to 35 nm), different PDMS block morphologies (cylinders and spheres), at different self-assembly stages and at different points in the etching process. An example concerning PDMS spheres is reported in Fig. 1 [3]. Before sphere revelation the GISAXS pattern reveal only very weak scattering signal even if spots are visible on both side of the beam-stop, which reveal the existence of domains. After sphere revelation the scattering signal drastically increases and clear scattering rods are observe evidencing a transition in the nanometric structure. In Fig. 1 (b) are represented the corresponding Scanning Electron Microscopy (SEM) images.

Also, the evolution of the GISAXS pattern during the thermal self-assembly of a monolayer of horizontal PDMS cylinders and of a monolayer of PDMS spheres in a PS matrix on silicon substrates could be measured. In Fig2, we report on the profile thermal annealing evolution during this self-assembly process in the case of horizontal cylinders in a PS matrix (PS-b-PDMS) is shown. A clear transition around 80 °C is observed between a micellar state of the thin layer (17 nm periodicity) and the cylindrical state (21 nm period).

Figure 3 shows PS-PDMS with a molecular weight of 45.5kg/mol after SVA on plane Spin-On-Carbon (SOC) surfaces without topography and the corresponding GISAXS profile showing a period of approximately 35nm after annealing. The PDMS cylinders are well aligned with a relatively high correlation length. The SOC surface has thus advantageous wetting behavior towards PS-b-PDMS making it unnecessary to treat the surface with polymer brushes or other functional layers.

PA26

DISTINCT PALM-LIKE DIFFUSE SHEETS FROM LAMMELLAR GRATINGS STUDIED WITH SMALL ANGLE SOFT X-RAY SCATTERING

A. Fernandez Herrero^{1,*}, V. Soltwisch¹, M. Pflüger¹, J. Probst² and F. Scholze¹

¹Physikalisch-Technische Bundesanstalt, Abbestr. 2-12, 10587 Berlin, Germany

²Helmholtz Zentrum Berlin, Albert-Einstein-Str. 15, 12489 Berlin, Germany

*analia.fernandez.herrero@ptb.de

The next generation of integrated circuits confront the increased importance of roughness effects due to the shrinking dimension of the structures. The effect of the roughness on the diffraction intensities has been a subject matter on the last decade and it was identified in several reports as a key parameter to consider for the reconstruction of such structures [1]. One of the major challenges in lithography is to measure and to characterize line width roughness (LWR) and line edge roughness (LER).

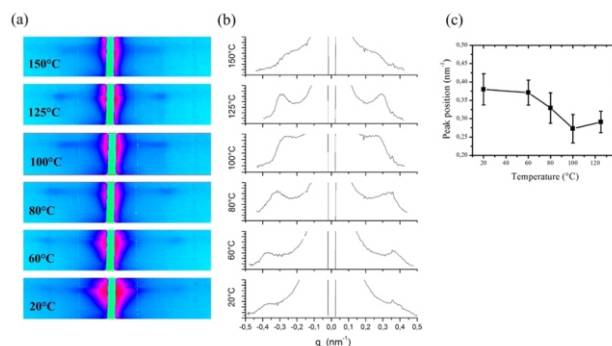


Figure 2. (a) Evolution of the GISAXS pattern of a thin layer (22 nm thick) of 21-nm pitch PS-PDMS during a thermal ramp evidencing a transition between a micellar and a horizontal cylindrical morphology around 80 °C, (b) intensity profiles along qy and (c) peak positions and standard deviations.

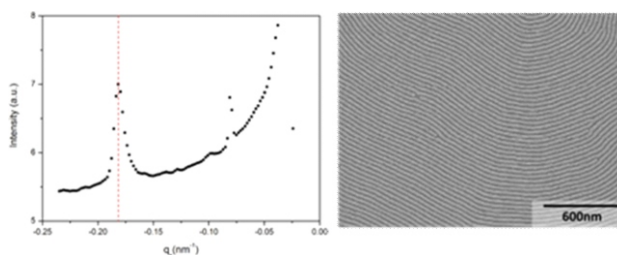


Figure 3. (left) GISAXS profile of SD45.5 on plane SOC surface, annealed for 75min in Toluene vapor. (right) SEM top view image of the same sample after plasma etching to reveal PDMS cylinders for SEM observation.

1. C. Girardot, S. Böhme, S. Archambault, M. Salaün, E. Latu-Romain, G. Cunge, O. Joubert, M. Zelsmann, *ACS Appl. Mat. Inter.*, **18**, (2014), 16276.
2. C. Sinturel, M. Vayer, M. Morris, M. Hillmyer, *Macromolecules*, **46**, (2013), 5399.
3. J. Garnier, J. Arias-Zapata, O. Marconot, S. Arnaud, S. Böhme, C. Girardot, D. Buttard, M. Zelsmann, *ACS Appl. Mater. Interfaces*, **8**, (2016), 9954.

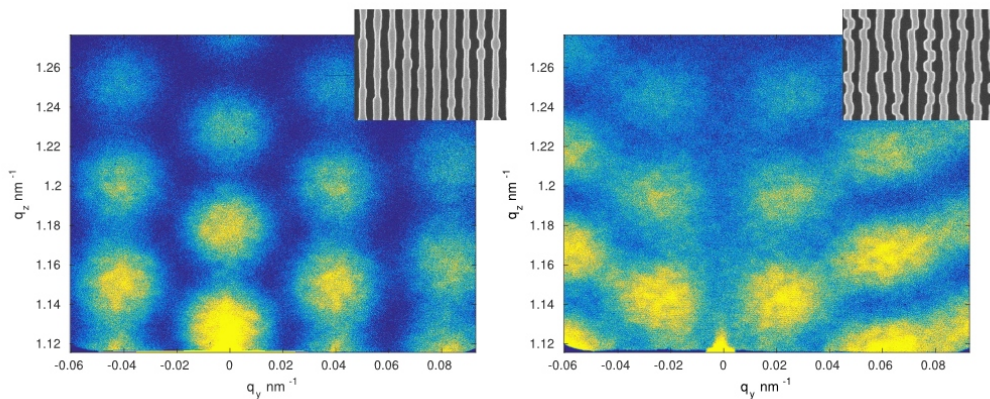


Figure 1. Diffuse scattering sheets from a sample with LWR (left) and LER (right). At the top right corners are the corresponding SEM image.

lows to distinguish directly between the nature of LER and LWR. This gives the opportunity of opening a new path for the characterization of LWR and LER.

1. Bartosz Bilski, Karsten Frenner, and Wolfgang Osten, "About the influence of Line Edge Roughness on measure defective-CD, *Opt. Express* **19**, 19967-19972 (2011).

2. A. Kato and F. Scholze, "Effect of line roughness on the diffraction intensities in angular resolved scatterometry," *Appl. Opt.* **49**, 6102-6110 (2010).

PA27

IN-SITU SYNCHROTRON STUDIES OF DENDRITE GROWTH IN SOLIDIFYING Ga-In ALLOYS

J. Grenzer¹, N. Shevchenko¹, O. Roshchupkina¹, C. Bähz¹, D. Hoppe¹, V. Cantelli^{1,2}, A. Rack² and S. Eckert¹

¹Helmholtz-Zentrum Dresden-Rossendorf, Dresden, Germany

²ESRF, Structure of Materials – ID19, 71 avenue des Martyrs, 38000 Grenoble, France
j.grenzer@hzdr.de

X-ray absorption contrast techniques are an important diagnostic tool to investigate solidification processes in metallic alloys. This work is devoted to an *in-situ* visualization of the dendrite growth during the bottom-up solidification of a Ga-25wt%In alloy under natural convection. The coupling of X-ray imaging with X-ray diffraction techniques provides additionally information of the crystallographic orientation of the growing dendrites.

Radiography / diffraction experiments were performed at BM20 and ID19 at the ESRF at a spatial resolution of $< 1 \mu\text{m}$. The temporal dynamics of morphological transitions such as retraction, coalescence and sidearm pinch-off were observed *in-situ*. Figure 1 shows an example of the sidearm shape evolution during a pinch-off process. The sidearm pinches off at the neck and the resulting fragment coarsens into a spheroid. The evolution of the morphological parameters like the neck radius was quantified by image processing and compared with numerical simulations. Figure 2 shows a diffraction image recorded in transmission geometry using an image plate detector. The fitted diffraction spots (black dots) on the left-hand side of the image are belonging to one particular orientation of the unit cell. The inset on the bottom right shows the corresponding orientation of the body-centered tetragonal *In* unit cell. One can see

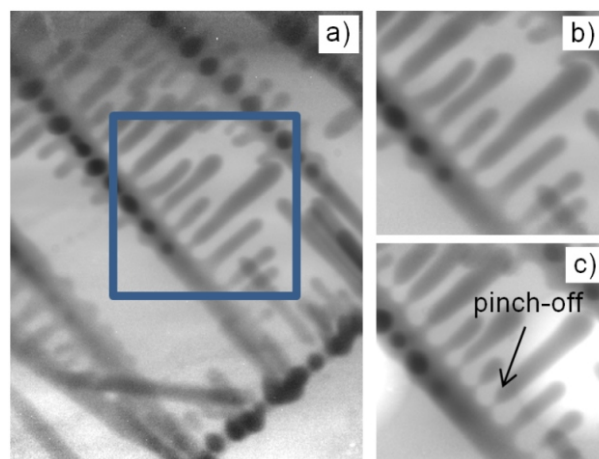


Figure 1. Radiography (spatial resolution $\sim 1 \mu\text{m}$): (a) selected dendrite, (b) sidearms and (c) pinch-off of the sidearms after ~ 90 minutes.

that the (110) orientation nicely fits to the orientation of the dendrite trunks (bottom left).

This *in-situ* technique offers a qualitative and even a quantitative description of the system behaviour: the composition and dendrite morphology evolution. Thus, these



in-situ experiments provide benchmark data that can be used to validate and improve existing micro-structural models.

This work is financially supported by the Helmholtz Association "LIMTECH". We would like to acknowledge the support of the Central Department of Research Technology @ HZDR.

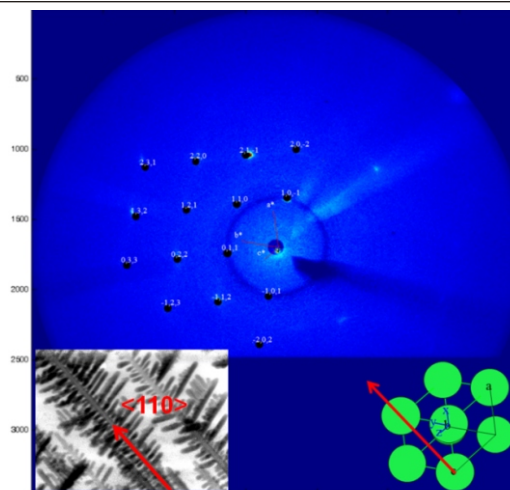


Figure 2. Diffraction at selected dendrites. Insets: dendritic structure (bottom left) and the corresponding orientation of the unit cell (bottom right).

PA28

STRUCTURAL CHANGES ACROSS THE METAL-INSULATOR TRANSITION IN THIN EPITAXIAL VO₂ FILMS

J. Grenzer¹, S. Facsko¹, X. Ou^{1,2}, Y. Ji¹

¹Helmholtz-Zentrum Dresden-Rossendorf, Institute of Ion Beam Physics and Materials Research, Ion Beam Center, Dresden, Germany

²State Key Laboratory of Functional Material for Informatics, Shanghai Institute of Microsystem and Information Technology, Chinese Academy of Sciences, 865 Changning Road Shanghai 200050 China
j.grenzer@hzdr.de

Vanadium dioxide (VO₂) got much interest in the recent years not only from the fundamental point of view as a correlated electron system but as well as due to its intriguing electrical and optical properties, like the metal-insulator transition (MIT) close to room temperature. This makes VO₂ favourable for optoelectronic, switching or even memory devices. The main challenge for device applications is the epitaxial growth of VO₂ on suitable substrates. Sapphire seems to be one of the promising substrate candidates for the growth of high quality epitaxial VO₂ phases.

Referring to literature, the MIT is directly connected with a change in the crystal structure, namely the transition from the low temperature monoclinic phase (P21/c) to the high temperature tetragonal (rutile) phase (P42/mnm). However, this symmetry change at the transition temperature should be strongly influenced by the epitaxy itself. Comparing our structural investigations and electrical measurements the results indicate that the MIT as observed by the resistance measurement in epitaxial VO₂ thin films seems to be not necessary accompanied by a complete monoclinic to rutile phase transformation. A slight lattice

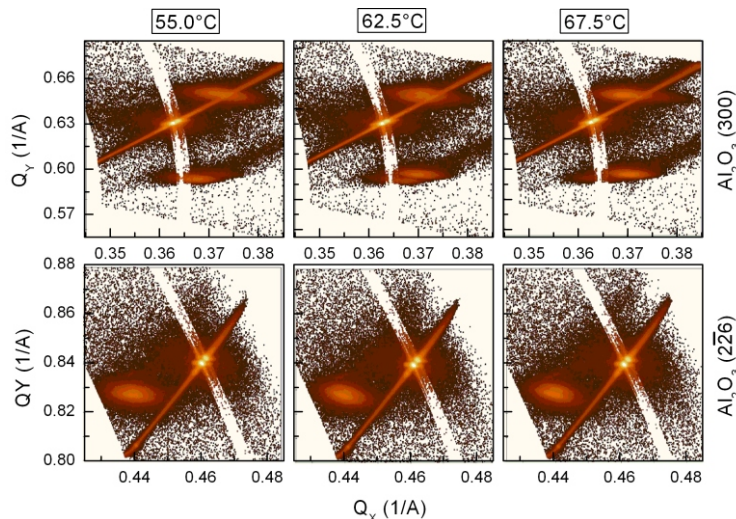


Figure 1. Change of the RSM's of the VO₂ thin film grown on a [1100] Al₂O₃ substrate as a function of temperature. The phase transition occurs at 62.5°C (see figure 2).

distortion causing a possible change in the atomic positions without breaking the existing the epitaxial relationship appears to be sufficient.

The support of I. Skorupa during sample preparation and of A. Scholz during the XRD measurements is acknowledged.

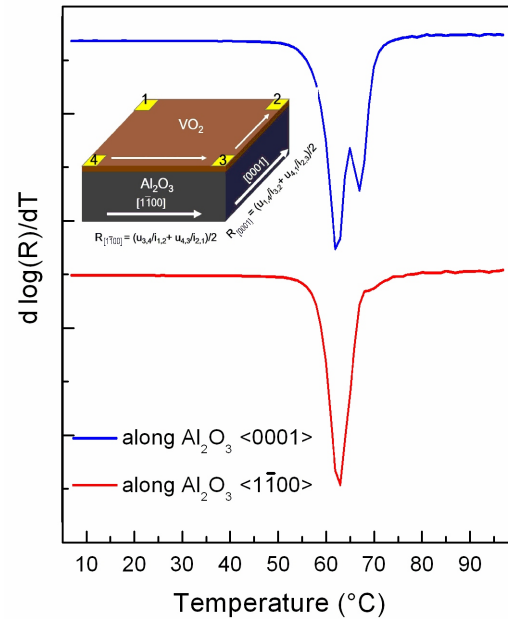


Figure 2. The corresponding electrical resistance measurements shows as well as an asymmetry a long diff. directions.

PA29

INCORPORATION OF INTERFACIAL ROUGHNESS TO RECURSION MATRIX FORMALISM OF DYNAMICAL X-RAY DIFFRACTION IN MULTILAYERS AND SUPERLATTICES

I. Lobach¹, A. Benediktovitch¹, A. Ulyanenkov²

¹Atomicus OOO, Minsk, Belarus

²Atomicus GmbH, Karlsruhe, Germany
igor.lobach@atomicus.by

High resolution x-ray diffraction is a powerful tool for the analysis of the multilayer epitaxial structures, and dynamical diffraction theory is usually used to reveal the physical properties of the investigated sample structure in finest details from the scattering pattern [1, 2]. The matrix formalism [2] delivers the algorithm for establishing the boundary conditions and describing the x-ray scattering process in a frame of dynamical theory. However, the standard realization of this algorithm does not take into account interfacial roughness, which is always present in multi-layered systems.

In this contribution, we consider interfacial roughness as a phenomenological transition layer with k_{0z} and k_{g0z} (Fourier components of crystal's susceptibility) and g_z (normal component of reciprocal lattice vector) as functions of z -coordinate, where z -axis is orthogonal to the multilayer's surface and directed downward. Two-wave dynamical diffraction theory in transition layers is found to be conveniently reformulated in the following form:

$$\frac{d}{dz} \begin{pmatrix} T \\ D \end{pmatrix} = i \begin{pmatrix} k_{0z} \frac{k_0^2}{2k_{0z}} \phi_0(z) & \frac{k_0^2}{2k_{0z}} \phi_g(z) \\ \frac{k_0^2}{2k_{g0z}} \phi_g(z) & k_{0z} \frac{k_0^2 - k_{g0}^2}{k_{g0z}} \phi_0(z) \end{pmatrix} \begin{pmatrix} T \\ D \end{pmatrix} \quad (1)$$

where \vec{k}_0 is the incident wave-vector, k_{g0} , k_0 , g_z in subscripts denotes z -components of the vectors, T and D have the following meanings: if one cuts out infinitesimal lamella with a coordinate z , thus producing a vacuum layer, then T and D are the amplitudes of down- and upward directed waves in this layer, respectively. The eq. (1) was resolved using special ansatz for T and D , having a form of solution for field in a single crystal with slowly varying amplitudes of two eigenwaves. An exact solution of eq. (1) is found for a certain type of transition layer and the universal iterative method of solution of eq. (1) has been developed, which proved to be sufficiently accurate even after single iteration (for realistic models of transition layers describing roughness). The analytical solution of eq. (1) enables to treat the transition layer as an additional matrix in the recursion matrix formalism [2]. The proposed approach is illustrated by numerical examples aiming to find the influence of the roughness on the diffraction profile.

1. A. Benediktovitch, I. Feranchuk and A. Ulyanenkov, *Theoretical Concepts of X-ray Nanoscale Analysis*, Springer, 2014.

2. S. A. Stepanov, E. A. Kondrashkina, R. Köhler, D. V. Novikov, G. Materlik and S. M. Durbin, *Phys. Rev. B*, **57**, (1998), 4829.



PA30

STRUCTURE OF SUPERCONDUCTING MgB₂ THIN FILMS ANNEALED IN OXYGEN

T. Roch¹, M. Gregor¹, T. Plecenik¹, L. Satrapinsky¹, M. Janík¹, M. Čaplovičová²,
A. Plecenik¹

¹Department of Experimental Physics, Faculty of Mathematics Physics and Informatics, Comenius University in Bratislava, Mlynska Dolina, 842 48 Bratislava, Slovakia

²Slovak Technical University, Center for Nanodiagnostics, Bratislava, Slovakia
roch@fmph.uniba.sk

After discovery of superconductivity of MgB₂ researchers have been investigating possibilities of improving its properties for usage in cryoelectronic and high-current applications. Among various approaches it was reported, that certain amount of impurities incorporated during thin film fabrication processes can act as pinning centres which may increase critical current density and the upper critical magnetic field. MgO is always present within MgB₂ film as the major impurity. Recently we have shown, that ex-situ annealing of vacuum co-evaporated MgB₂ thin films in Ar and N₂ atmospheres at 700 Pa and up to 800°C produces relatively thick MgO layer on the film surface [1]. Annealing in Ar+5%H₂ atmosphere strongly suppresses creation of the oxide layer. Interestingly samples with the thickest MgO on the surface showed the highest T_c=34.8 K with sharp transition T~0.1 K. XPS and XRD measurements suggest that the MgO serves as protecting top layer which prevents outdiffusion of Mg from films during annealing and leads to improved MgB₂ stoichiometry and larger grain size.

In consequent research we have studied effect of annealing in pure oxygen atmosphere. MgB₂ thin film annealed in O₂ (5.0) at 700 Pa and at 800°C exhibited improved superconducting critical temperature of 35.6 K, high critical current density of 2.4 x 10⁷ A/cm² and the upper -critical field H_{c2}(0) of 31 T.

The chemical composition depth profiles of the thin films were measured by X-ray photoelectron spectroscopy. Structure was investigated using PANalytical X'pert PRO MRD diffractometer with CuK radiation and transmission electron microscopy (TEM) with selected area electron diffraction (SAED). Detailed measurement showed 200 nm thick MgO layer developed on top of 300 nm thick MgB₂ with the typical grain size around 15 nm (Fig 1). The presence of about 6% oxygen within MgB₂ suggests MgO phase beside MgB₂. In oxygen annealed sample extra MgO can serve as flux pinning centres. Detailed texture measurements show biaxial texture with respect to c-cut Al₂O₃ substrate: MgO(111)[1-10] || Al₂O₃(0001) [1-100]. Beside certain random amount, MgB₂ phase showed single axis texture with the (001) axis inclined at 14° with respect to surface normal Al₂O₃(0001). This was revealed also in measurement of pole figure 101 MgB₂ as shown in Fig.2. Single axis textured pure Mg phase with the same inclination angle has been observed in pole figures of 001 and 100 Mg. In addition there exists a minor non-determined Mg-B(O) phase showing exceptional biaxial texture. Structural data help to understand special anisotropic superconductivity in the annealed films. Any extra phase in-

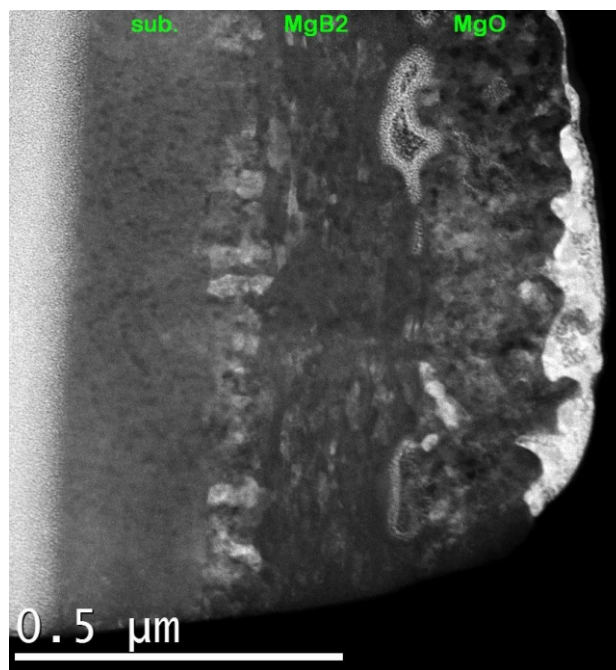


Figure 1. TEM of the sample annealed in O₂.

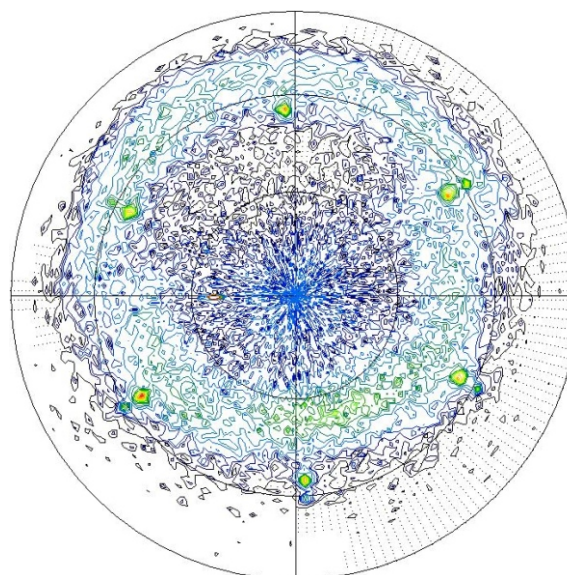


Figure 2. Texture pole figure measured in 101 MgB₂ (diffuse intensity in shifted circular form). MgO oriented phase exhibits six regular maxima 200 accompanied by substrate artefacts.

fluences special intergranular coupling between MgB₂ grains which has impact on superconducting properties of film.

1. M. Gregor, T. Plecenik, R. Sobota, J. Brndiarova, T. Roch, L. Satrapinsky, P. Kus, A. Plecenik, *App. Surf. Sci.*, **312**, (2014), 97.

Authors would like to acknowledge a support by the Research & Development Operational Program funded by

EDRF supporting the project implementation: ITMS 26220220004. The work was also supported by the Slovak Research and Development Agency under Contract No. APVV-494-11.

PA31

NUMERICAL MODELLING OF REFLECTIVE MULTILAYER BASED X-RAY OPTICS

P. Piault¹, C. Ferrero¹, F. Delmotte², S. Berujon¹, A. Rack¹, C. Morawe¹, J. P. Guigay¹, E. Ziegler¹

¹ ESRF – The European Synchrotron, CS40220, 38043 Grenoble cedex 9, France

² Laboratoire Charles Fabry, Institut d'Optique Graduate School, CNRS, Université Paris-Saclay, 91127 Palaiseau Cedex, France
pierre-etienne.piault@esrf.fr

The ESRF upgrade programme launched in May 2015 aims to build an Extremely Brilliant Source (EBS) capable of producing more intense, coherent and stable X-ray beams. ESRF EBS bears several challenges for synchrotron instrumentation. One of them is to build flawless optics, i.e. optics capable to either propagate a perfect wavefront from the source to the sample without degradation or to correct for the wavefront imperfections. Artificially stratified films deposited on a mirror surface are envisaged as optical elements for these purposes.

Multilayer mirrors exhibit several attractive reflection properties compared to crystals, e.g. the possibility to enlarge the energy bandwidth at X-ray wavelength by two orders of magnitude. Another possibility is the ability of defining on demand the Bragg angle by varying the deposited layers' thickness, which is particularly interesting for wavelengths above 1 nm. On the other hand, multilayer-coated mirrors have shown to degrade the beam coherence and distort the reflected wavefront. This can cause a loss of sensitivity by blurring effects while the propagation of phase distortions may result in the presence of undesired intensity variation in the recorded images in the form of stripe-line modulations perpendicular to the diffraction plane (Fig. 1B and Fig. 2). The origin of such intensity modulations remains under discussion.

Significant efforts were made to minimise the degradation of the X-ray beam coherence upon multilayer reflection [1-3]. Studies involving multilayers made of various material compositions and coating parameters produced by different deposition facilities [2] lead to the observation of unwanted stripes of diverse intensities in the reflected beam and to a degradation of the coherence properties. Currently, the most likely interpretation for that is based on the explanation already given for silicon mirrors, i.e. imputing the wave distortion to the height deviation from a perfect surface [4-6]. Hence, the substrate quality may strongly affect the performance of the multilayer coating [3]. This problem may get rapidly complex if one tries to consider the role of every layer in the coating. Questions also arise regarding the spatial frequency range that influences the stripe patterns. The difference between correlated and uncorrelated layer waviness may also be taken into account.

To address these issues the following project was initiated:

Firstly, images of W/B₄C multilayers were characterised at the ESRF instrumentation beamline BM05. In this experiment (Fig. 1) the reflected monochromatic beam was recorded at various distances to detect a possible dependence of the stripes on the figure errors of the multilayer. Further experiments were performed to gain an insight into

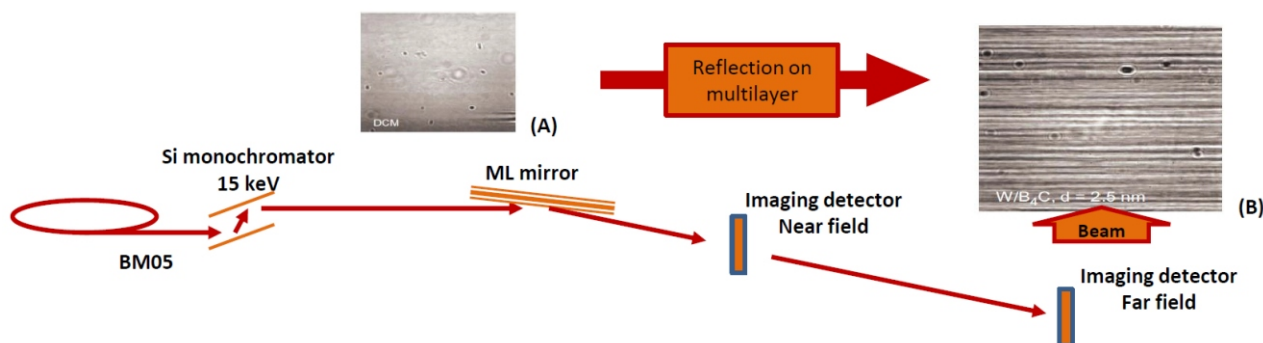


Figure 1. Experimental setup for multilayer characterisation at BM05. (A) Image of the beam after diffraction from a double crystal monochromator. (B) Image of the beam reflected by a W/B₄C multilayer.

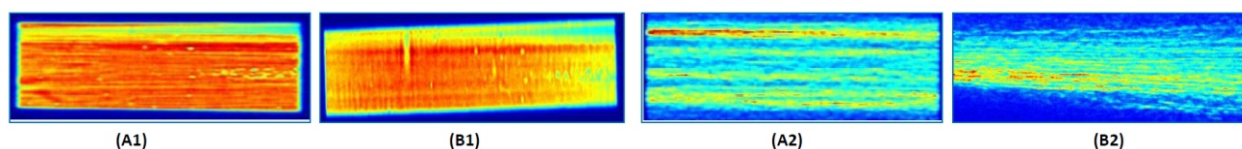


Figure 2. Reflected beam from the used multilayers at a 6.5 m distance from the mirror. Sample M1: $[W/B_4C]_{60}$, d-spacing = 4 nm, sample M2: $[W/B_4C]_{20}$, d-spacing = 4 nm. (A1) and (A2): reflections in the vertical plane for M1 and M2, respectively. (B1): reflection in the horizontal plane for M1. (B2): reflection in the vertical plane for M2 turned by 90° with respect to the incoming beam.

the way X-rays propagate in a multilayer in order to build an effective model for the multilayer reflection. For example, the orientation of the multilayer was flipped from the vertical to the horizontal position for investigating the effect of the transverse coherence length of the diffracted beam on the image pattern (Fig. 2). The beam wavefront shape was recovered using a speckle metrology technique [7].

Secondly, we started developing a numerical model capable of simulating the beam reflected by a multilayer. For a comprehensive simulation of the layered medium, topographies of the multilayer coating and/or substrate surfaces as recorded by Fizeau interferometry will be needed. The model should provide height deviation maps as well as X-ray profiles propagating in the multilayer. Our first approach consisted in modifying a model based on the Takagi-Taupin equations developed originally for a perfect flat or elliptical multilayer. In this case, the height deviations are implemented as a suitable offset of the susceptibility function of the layered medium.

First experimental results (Fig. 2) show the stripes observed after reflection on multilayers in the horizontal and vertical plane, respectively. By changing the orientation of the multilayers with respect to the incoming beam and as well their distance to the detector, it is possible to separate the contributions of the beam features (Fig. 2 A1 and B1) and of the stated isotropy of the height deviations (Fig. 2 A2 and B2).

PA32

CHARACTERIZATION OF TITANIUM AND TITANIUM (IV) OXIDE NANOFILMS WITH X-RAY REFLECTOMETRY AND GRAZING INCIDENT X-RAY DIFFRACTION

I. Stabrawa¹, D. Banaś^{1,2}, A. Kubala-Kukuś^{1,2}, M. Pajek¹, U. Majewska^{1,2},
J. Wudarczyk-Moćko² and S. Gózdź^{2,3}

¹Institute of Physics, Jan Kochanowski University, Świętokrzyska 15, 25-406 Kielce, Poland

²Holycross Cancer Center, Artwińskiego 3, 25-734 Kielce, Poland

³Institute of Public Health, Jan Kochanowski University, Al. IX w. Kielc 19, 25-317 Kielce, Poland
ilona.stabrawa@interia.pl

In recent years, titanium and titanium alloys have been widely used in the medical devices due to their excellent corrosion resistance, good biocompatibility and mechanical properties [1]. Titanium (IV) oxide is a highly efficient in killing antibiotic resistant bacteria, i.e. methicillin-resistant *S. aureus* (MRSA), and highly resistant to UV light bacteria such as *Enterobacter cloacae*. Most of these bacte-

The ultimate goal of this work, still in progress, is to explore and eventually propose ways to improve the quality of multilayer mirrors for forthcoming applications in present and future X-ray source facilities.

1. A. Rack, T. Weitkamp, M. Riotte, D. Grigoriev, T. Rack, L. Helfen, T. Baumbach, R. Dietsch, T. Holz, M. Krämer, F. Siewert, M. Meduna, P. Cloetens, E. Ziegler. *J. Synchrotron Rad.* 17, (2010), 496–510.
2. A. Rack, L. Assoufid, W.-K. Lee, B. Shi, C. Liu, Ch. Morawe, R. Kluender, R. Conley, N. Bouet. *Radiat. Phys. Chem.* 81 (2012) 1696-702.
3. C. Morawe, R. Barrett, K. Friedrich, R. Klünder, A. Vivo. Spatial coherence studies on x-ray multilayers. In: C. Morawe, A.M. Khounsary, S. Goto. (Eds.) *Advances in X-Ray/EUV Optics and Components VI*, Proceedings of SPIE, (2011) vol. 8139, p. 813909.
4. P. Cloetens, R. Barrett, J. Baruchel, J.-P. Guigay. & M. Schlenker. *J. Phys. D*, 29, (1996). 133–146.
5. E. Ziegler, C. Morawe, O. Hignette, P. Cloetens. & R. Tucoulou. *Ninth International Conference on Production Engineering*, Osaka, Japan, (1999) pp. 285–291.
6. K. Yamauchi, K. Yamamura, H. Mimura, Y. Sano, A. Saito, K. Endo, A. Souvorov, M. Yabashi, K. Tamasaku, T. Ishikawa, Y. Mori. *Appl. Opt.* 44, (2005). 6927–6932.
7. S. Berujon, H. Wang, and K. Sawhney *Physical Review A* 86, (2012) 063813.

ria occur in water, sewage, soil, meat, hospital facilities as well as on the skin and in the mouth [2].

In this work the X-ray reflectometry (XRR) [3] and grazing incident X-ray diffraction (GIXD) were applied to analysis and characterization of surfaces in the form of titanium and titanium (IV) oxide nanofilms. The X-ray reflectometry (XRR), which uses the effect of total external reflection of X-rays, is surface sensitive analytical tech-

nique used for investigation of the near surface regions of thin films. This technique allows modeling of thin layers density, thickness and roughness of the surface and the substrate and was already successfully applied by our group for determination of physical properties of a gold nanolayers [4] used later for biomolecule-metal surface interaction studies. The method of grazing incident X-ray diffraction (GIXD) [5] is a modification of standard X-ray diffraction technique, which due to low incident angle of the X-ray beam maximizes signal from the surface and as a result allows for phase analysis on thin layers and depth profiling of the phase composition of layered samples.

The studied nanofilms, with thicknesses 25, 50 and 75 nanometers, were prepared by evaporation of titanium and titanium (IV) oxide on different substrates: glass, quartz and crystalline silicon. The measurements were performed using X'Pert Pro MPD diffractometer/reflectometer equipped with copper anode x-ray tube and X'Celerator strip detector.

PA33

FULL STRAIN TENSOR DETERMINATION IN SYNTHESIZED DIAMONDS AND DIAMONDS FILMS

I. Fodchuk¹, M. Borcha¹, V. Khomenko¹, S. Balovsyak¹, V. Tkach², O. Statsenko²

¹Yuriy Fedkovych Chernivtsi National University, Chernivtsi, Ukraine

²V. Bakyl Institute for Superhard Materials of NASU, Kyiv, Ukraine
m_borcha@ukr.net

The synthesis of diamond crystals with high degree of crystalline perfection at the comparative low parameters (temperature and pressure) is possible due to the *C-Mg* synthesis system. However crystals synthesized in such system are unstable. Synthesis pressure and temperature can be reduced to 7.7 GPa and 1700 °C, respectively, with adding *Ni* to the *C-Mg* system. At the same time, the *Mg* and *Ni* elements changes electric and optical properties of crystals in dependence on their content. It has the practical application, in particular, in an electronic devices, in optical filters and devices for measuring the absorbed radiation power.

The method of electron backscattering diffraction (the Kikuchi method) is the effective method for determination of the local strains in monocrystalline materials, polycrystalline films and multilayer structures. High spatial resolution and locality are proper to this method owing to the newest CCD detectors.

We present technique of full strain tensor determination from Kikuchi patterns and it application to diamond crys-

The motivation of the experiment, physical basis of the methods used, experimental setups, results of optimization of the measurement procedure and results of the measurements for titanium and titanium (IV) oxide surfaces of different thicknesses evaporated on different substrates will be presented.

1. A. Markowska-Szczupak, K. Ulfig, A.W. Morawski, *Catalysis Today*, 169, (2011), 249-257.
2. M. Chen, E. Zhang, L. Zhang, *Materials Science and Engineering: C*, 62, (2016), 350-360.
3. L. G. Parratt, *Physical Review*, 95, (1954), 359-369.
4. I. Stabrawa, D. Banaś, K. Dworecki, et al., *Acta Physica Polonica A*, 129, (2016), 233-236.
5. J. Als-Nielsen, J. Jacquemain D. Kjaer, et al., *Physics Reports*, 246, (1994), 251-313.

tals synthesized in the *C-Mg* system with adding *Ni* as well as polycrystalline diamond films. This technique consists in comprehensive analysis of Kikuchi pattern: displacements of crystallographic zone axes (intersections of Kikuchi bands), width of Kikuchi bands, intensity distributions across Kikuchi band, Fourier transformation and cross-correlation methods. All component of strain tensor were determined for each grain of researched samples. For instance, it is shown that all grains of diamond crystal have approximately equal values of shear components ϵ_{xz} and ϵ_{yz} , that testifies the absence of rotation in corresponding crystallographic directions, at the same time, other components considerable variate from grain to grain.

1. M.D. Borcha, S.V. Balovsyak, I.M. Fodchuk, V.Yu. Khomenko, V.N. Tkach, *Journal of Superhard Materials*, 35, No. 4, (2013), 35.
2. A. Wilkinson, B. Britton, *Materials Today*. 15, N 9, (2012), 366.



PA34

STRUCTURE DIAGNOSTICS OF HETEROSTRUCTURES AND MULTILAYERED SYSTEM BY X-RAY MULTIPLE DIFFRACTION

M. Borcha¹, I. Fodchuk¹, M. Solodkyi¹, M. Baidakova², G. Klimko², I. Sedova²,
R. Sokolov², S. Sorokin², M. Yagovkina²

¹*Yuriy Fedkovych Chernivtsi National University, Chernivtsi, Ukraine*

²*loffe Physical-Technical Institute of the Russian Academy of Sciences, St.-Petersburg, Russia*
m_borcha@ukr.net

The X-ray multiple diffraction [1-2] is a precision tool for determination of the lattice parameters and the strain distribution in complex systems and crystalline materials [3]. It was shown by means of calculations of multiple X-ray diffraction patterns [1] that the accuracy of this method can be increased if the conditions of coplanar three-beam or noncoplanar four-beam diffraction are realized.

In this report we present the researches of multilayered heterostructures by a modified calculating technique of multiple X-ray diffraction. It provides an opportunity to choose appropriate conditions for each layer of the heterostructure to implement the specific cases of multiple diffraction, in particular, coplanar three-beam or coincidental noncoplanar four-beam diffraction [1].

Approbation of this technique was conducted with experimental Renninger scans from heterostructures and Zn(Mn)Se/GaAs(001) multilayered system. It is shown that the implementation of noncoplanar four-beam diffraction for θ can be associated with a specific value of x and geometric conditions. In particular, for CoK₁-radiation when $x = 7.5\%$ superposition of θ and three-beam maxima leads to minimization of instrumental factor influence. Values of $a/\lambda = 3.607428$ and, consequently, $a = 6.45358 \text{ \AA}$, were obtained from the calculations. Thus, the accuracy of a is determined by θ accuracy only.

On the other hand, using advantages of the synchrotron radiation spectral range is not difficult to satisfy the condition of the three-beam coplanar diffraction for any x . For instance, for $x = 10.5\%$ at $\lambda = 1.78611 \text{ \AA}$ lattice parameter is $a = 6.443265 \text{ \AA}$. This provides the conditions for effective control of the chemical composition and strain distribution with high precision during the heterostructures growth.

At the same time, in the case of a Zn(Mn)Se/GaAs(001) multilayered system the degree of tetragonal lattice distortions i.e. the relationship between a and a_{\parallel} in each layer were determined from the analysis of the dynamics of the individual multi-beam maxima, which have different behaviour at lattice deformation (compression or stretching) because direction of peak displacement depends on the sign of the strain. It gives possibility to establish how the Mn component is included to lattice: substituting Zn or Se, or generating interstitial point defects.

1. M. Borcha, I. Fodchuk, I. Krytsun, *Physica status solidi A*, **206**, 8, (2009), 1699.
2. V.G. Kohn, *J. Moscow Phys. Sos.*, **1**, (1991), 425.
3. S. L. Morelhao, L. H. Avanci, A. A. Quivy, E. Abramof, *J. Appl. Cryst.* **35**, (2002), 69.

PA35

DEFECT STRUCTURE OF HIGH-RESISTANT CdTe CRYSTALS STUDIED BY HIGH-RESOLUTION X-RAY DIFFRACTION

I. Fodchuk¹, I. Gutsuliak¹, V. Dovganyuk¹, M. Solodkyi¹, O. Maslyanchuk¹, Yu. Roman¹,
N. Safriuk², V. Kladko², M. Barchuk³

¹*Chernivtsi National University, Kotsjubynskyyi str. 2, Chernivtsi, Ukraine*

²*Institute of Semiconductor Physics of NASU, Nauky str. 41, Kyiv, Ukraine*

³*Institute of Materials Science, TU Bergakademie Freiberg, Gustav-Zeuner-Str. 5, Freiberg, Germany*
ifodchuk@ukr.net

Cadmium telluride (CdTe) is one of the most promising materials for highly efficient detectors of X- and γ -radiation working without cryogenic cooling with sensitivity extended to the region of high photon energies compared with Si detectors [1,2]. The series of MoO_x/p-CdTe (111)-oriented heterostructures with different degrees of imperfection manufactured by reactive magnetron sputter-

ing was chosen for our research. The experimental investigations in different X-ray diffraction geometries (symmetrical 333, forbidden 222 reflections as well as asymmetrical one 331) were performed on Philips X'Pert PRO diffractometer.

The samples are known to possess different types of defects namely dislocation loops, Lomer-Cottrell junction, inclusions etc. Therefore, the simulation of reciprocal

space maps (RSM) for (333) and (331) reflections were performed using the model of real crystal, which contains complexes of structural defects [3]. The influence of this system on the diffraction pattern is comparable to the set of edge dislocations with dislocation lines perpendicular to the surface plane and different directions of Burgers vector in this plane: $a/2[110]$ and $a/2[1\bar{1}10]$. The density of these dislocations was determined as $2.86 \times 10^6 \text{ cm}^{-2}$ and $2.38 \times 10^6 \text{ cm}^{-2}$. In particular, a case of stacking faults was considered according to which a large dislocation loop restricts the region with small point defects and inclusion of another phase. The characteristic intensity distribution around reciprocal space nod indicates the presence of individual blocks separated by small-angle boundaries with the angle of misorientation about 0.5 degrees.

It is worth to note that several samples have block structure as evidenced by the emergence of several diffraction maxima placed at the same Q_z value on RSM (Fig. 1a). The calculated RSMs (Fig 1.b) correlate well with the experimental ones that indicates the correctness of the chosen defects model.

1. S.D. Sordo, L. Abbene, E. Caroli, A.M. Mancini, A. Zappettini, and P. Ubertini. *Sensors*, **9** (5), (2009), 3491.
2. C. Szeles. *Phys. Stat. Sol. (b)* **241** (3), (2004), 783.
3. C. Sun, T. Paulauskas, F. G. Sen, G. Lian, J. Wang, C. Buurma, M. K. Y. Chan, R. F. Klie, M. J. Kim. *Scientific Reports*, **6**, (2016), 27009.

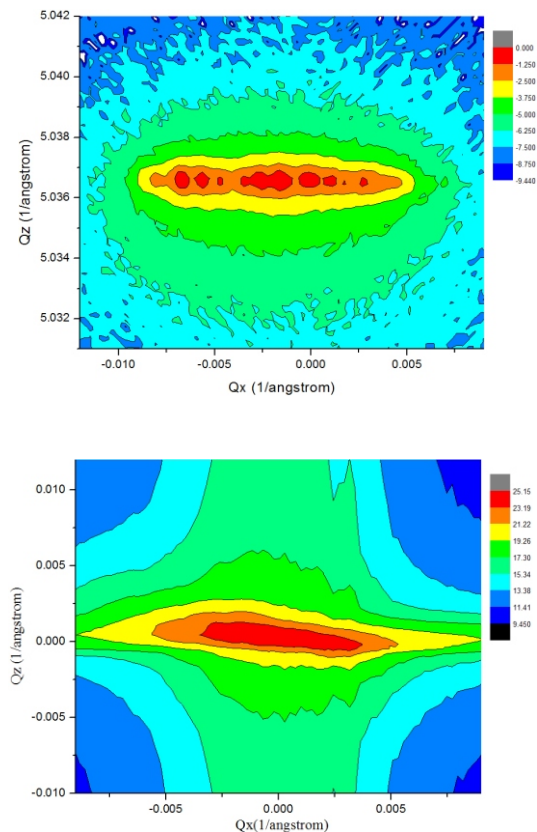


Fig. 1. Experimental (top) and calculated (bottom) RSM, in 333 reflection.

PA36

DEFECT AND MAGNETIC STRUCTURE OF $\text{Y}_{2.95}\text{La}_{0.05}\text{Fe}_5\text{O}_{12}/\text{Gd}_3\text{Ga}_5\text{O}_{12}$ EPITAXIAL SYSTEMS

I. Fodchuk¹, I. Gutsuliak¹, V. Dovganyuk¹, A. Kotsyubynskiy¹, N. Safriuk², P. Lytvyn², V. Kladko², M. Barchuk³, I. Syvorotka⁴

¹Chernivtsi National University, Kotsyubynskiyi str. 2, Chernivtsi, Ukraine

²Institute of Semiconductor Physics of NASU, Nauky str. 41, Kyiv, Ukraine

³Institute of Materials Science, TU Bergakademie Freiberg, Gustav-Zeuner-Str. 5, Freiberg, Germany

⁴Scientific Research Company "Carat", Strijska str. 202, Lviv, Ukraine

ifodchuk@ukr.net

The set of complementary techniques such as high-resolution X-ray diffraction, atomic force microscopy (AFM), and magnetic force microscopy (MFM) supported by simulation were used to investigate $\text{Y}_{2.95}\text{La}_{0.05}\text{Fe}_5\text{O}_{12}$ yttrium iron garnet (YIG) epitaxial films of different thicknesses ranging from 2.3 to 94.4 μm . We performed a series of reciprocal space maps (RSM) calculations taking into account a presence of the sample/substrate interlayer and changing the density of dislocations. The influence of a film perfection on microstructure of magnetic domains and the RSM's shapes was studied.

From the MFM analysis, it follows that the magnetic domain structure depends on the layers thickness. For the thinnest samples (2.3 μm), we revealed disordered stripe-shaped approximately 1 μm wide domains accompanied by

frequent breaks and bubble domains, which appear because of influence of highly distorted regions close to the interface. The sample with the middle thickness (6.4 μm) possesses continuous parallel stripes with the periodicity of approximately 11 μm and some heterogeneity caused by small thickness of the film, which disappears with the overgrowth [1]. The stripes observed in thicker samples (above 70.7 μm) have a chaotic heterogeneous structure and varying width, which is typical for the films with well-formed column structure.

Experimental rocking curves and RSMs were recorded in symmetrical (444), (888) and asymmetrical (880) reflections at high-resolution X-ray diffractometer X'Pert PRO MRD. The RSMs of the thinnest sample (2.3 μm) contain



two peaks stemming from the film and the substrate. The contribution of the latter to the diffraction pattern is significant, while the structure of the film is highly distorted due to its small thickness. The sample with the thickness of 6.41 nm has a well-formed crystal structure. An additional peak from the film–substrate transition layer is observed on the map along q_z axis. Along q_x axis, the map is asymmetrical, which indicates a presence of the misfit dislocations oriented in (100) plane. The RSM shapes of other samples are typical for a high content of inclusion defects and dislocation loops of small sizes in the near-surface layer, which is a common feature of selected growth conditions.

The simulation of RSMs is based on the kinematical theory described by Krivoglaz [2] and performed using Monte-Carlo approach [3]. Two sets of screw and edge dislocations with different densities were selected as the dom-

inant type of defects. Their density was determined as 10^5 – 10^8 cm⁻². Alternatively, the dislocation loops with the sizes of 2–5 nm were defined from RSMs, which density depends on the sample thickness. We achieved a good correspondence between simulated and experimental RSMs. It was established that the stripe domain structure of garnets depends drastically on the samples thickness, roughness of the surface and film growth conditions.

1. I. Fodchuk, I. Gutsuliak, V. Dovganiuk, A. Kotsyubynskiy, U. Pietsch et al. *Appl. Opt.* **55**, (2016), B144.
2. M. A. Krivoglaz, *X-Ray and Neutron Diffraction in Nonideal Crystals*. Berlin: Springer. 1996.
3. M. Barchuk, V. Holy, B. Miljevic, B. Krause, T. Baumbach et al. *J. Appl. Phys.* **108**, (2010), 043521.

PA37

X-RAY REFLECTOMETRY AND SCATTERING STUDY OF THE SURFACE NANOLAYERS ON COLLOIDAL SILICA

B. S. Roshchin¹, A. M. Tikhonov², Yu. O. Vokov¹, V. E. Asadchikov¹, A. D. Nuzhdin¹

¹A. V. Shubnikov Institute of Crystallography of Federal Scientific Research Centre "Crystallography and Photonics" of Russian Academy of Sciences, Leninsky prospekt, 59, Moscow 119333, Russia

²P. L. Kapitza Institute for Physical Problems of Russian Academy of Sciences, Kosygina street, 2, Moscow, 119334, Russia
ross@crys.ras.ru

We report the results of X-ray study of surface nanolayers on colloidal silica which obtained by modification of silica by different alkali ions and by deposition of polar lipids on the surface. Colloidal silica consists of monodisperse silicon oxide nanoparticles dissolved in water. Due to the high charge of these nanoparticles the surface of colloidal silica is highly polarized. Thereby electrical double layer near its surface is formed [1]. Applying the model-independent approach for experimental data fitting [2] we performed the reconstruction of depth-profile of the dielectric constant for silica sols which for different size of silicon oxide nanoparticles. The thickness dependence of near surface electrical double layer from the size of silicon oxide nanoparticles is revealed. The changes of the layer parameters after colloidal silica sample preparation are also studied. The presence of levitating ions layer for silica modified by alkali ions is found.

A phospholipid bilayer on liquid substrate can be considered as the simplest model of a cell membrane [3]. We used the method of preparation of macroscopically flat regular lipid multilayers described in [4]. The multilayer of 1,2-distearoyl-sn-glycero-3-phosphocholine (DSPC) was studied by both X-ray reflectometry and scattering using the diffractometer with a mobile tube-detector system [5].

Using the same approach [2] the spontaneous ordering effect of the multilayer structure is shown. Scattering diagrams correspond to the case of correlated interfaces in the multilayer [6].

1. A. M. Tikhonov, *J. Phys. Chem. C*, **111**, (2007), 930
2. I. V. Kozhevnikov, *Nucl. Instr. Meth. Phys. Res. A*, **508**,(2003), 519.
3. D. M. Small, *The Physical Chemistry of Lipids*. New York: Plenum press. 1986.
4. A. M. Tikhonov, *JETP Letters*, **92**, (2010), 394.
5. V. E. Asadchikov, V. G. Babak, A. V. Buzmakov, Yu. P. Dorokhin, I. P. Glagolev, Yu. V. Zanevskii, V. N. Zryuev, Yu. S. Krivonosov, V. F. Mamich, L. A. Moseiko, N. I. Moseiko, B. V. Mchedlishvili, S. V. Savel'ev, R. A. Senin, L. P. Smykov, G. A. Tudosi, V. D. Fateev, S. P. Chernenko, G. A. Cheremukhina, E. A. Cheremukhin, A. I. Chulichkov, Yu. N. Shilin, V. A. Shishkov, *Instruments and Experimental Techniques*, **48**, (2005), 364.
6. I. V. Kozhevnikov, *Nucl. Instr. Meth. Phys. Res. A*, **498**,(2003), 482.

This work was supported by Russian Foundation for Basic Research, project #15-32-20935.

PA38

SYNTHESIS, CRYSTAL STRUCTURE STUDIES AND VALIDATION USING X-RAY POWDER DIFFRACTION COMBINED WITH DFT CALCULATIONS OF BIOACTIVE DERIVATIVES

EISayed M. Shalaby^{1,3}, Adel S. Girgis² and Andy Fitch¹

¹European Synchrotron Radiation Facility, CS40220, 38043 Grenoble Cedex 9, France

²Pesticide Chemistry Department, National Research Centre, Dokki, Giza 12622, Egypt

³X-Ray Crystallography Lab., Physics Division, National Research Centre, Dokki, Giza 12622, Egypt
shalaby@xrldlab-nrc-eg.org

Two 3-(arylmethylidene)pyrrolidin-2,5-diones, **3a** and **3b**, were synthesized and characterized by powder X-ray diffraction since growing suitable single crystals were not successful. High-resolution synchrotron X-ray powder diffraction data were collected at room temperature at ID22 beamline at the European Synchrotron Radiation Facility (ESRF), Grenoble, France. The molecular structures were studied by theory using AM1, PM3 and DFT. The basic difference between the theoretical and experimental structures was found in the relative orientation of phenyl and chlorophenyl rings with respect to the central pyrrolidin-2,5-diones.

1. Girgis AS, Aziz MN, Shalaby EM, Saleh DO, Mishriky N, El-Eraky WI, et al. Molecular structure studies of novel bronchodilatory-active 4-azafluorenes. *Zeitschrift für Krist - Cryst Mater* 2016 Jan 1.231(3). Available from: <http://www.degruyter.com/view/j/zkri.2016.231.issue-3/zkri-2015-1892/zkri-2015-1892.xml>.

2. Moustafa AM, Girgis AS, Shalaby SM, Tiekink ERT. 1'-Methyl-4'-(4-methyl-phen-yl)dispiro-[indane-2,3'-pyrrolidine-2',3''-indoline]-1,2''-dione. *Acta Crystallogr Sect E Struct Rep Online* [Internet]. 2012 Jul 1. [cited 2015 May 24];68(Pt 7):o2197-8. Available from: <http://scripts.iucr.org/cgi-bin/paper?QM2073>.

The authors are grateful for financial support from the Science and Technological Development Fund (STDF) and the Institut Français d'Egypte (IFE) (Project 17408). We thank the ESRF for provision of experimental time on beamline ID22.

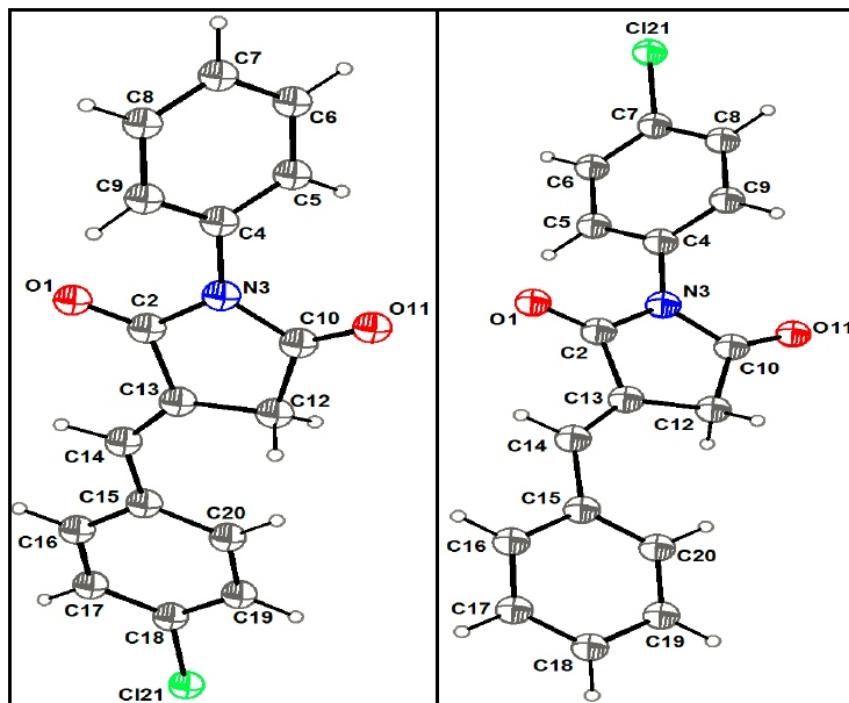


Figure 1: A view of the structures of **3a** (left) and **3b** (right), showing the atom-labeling scheme. Displacement ellipsoids are drawn at the 50% probability level.



PA39

X-RAY DIFFRACTION STUDIES OF CUBIC GaN EPILAYERS GROWN ON 3C-SiC/Si

M. Frentrup, S.-L. Sahonta, M.J. Kappers, C.J. Humphreys, D.J. Wallis

University of Cambridge, Department of Materials Science and Metallurgy,
27 Charles Babbage Road, Cambridge, CB3 0FS, United Kingdom
mf562@cam.ac.uk

GaN-based LED and laser heterostructures grown in the hexagonal wurtzite phase along the (0001) *c*-orientation feature large internal electrical fields, which can cause a reduction of the optical efficiency [1]. To overcome this problem, growth along so called semi- and nonpolar orientations, in which these fields are reduced or absent, has been investigated by numerous groups. Another promising approach is the growth of GaN in the cubic zincblende structure with (001) orientation, in which no internal polarisation fields are present. Furthermore the smaller bandgap of cubic nitrides require less Indium in InGaN quantum wells for green wavelength emission [2].

As *zincblende GaN* is *metastable* at normal growth temperatures and pressures, such epilayers tend to incorporate energetically preferred wurtzite-type inclusions and stacking faults.

In our poster presentation we will describe the structural characterisation of cubic GaN epilayers grown on 3C-SiC/Si (001) substrates using X-ray diffraction (XRD) techniques. *Texture maps*, which are projections of X-ray reflection distributions in reciprocal space on a two dimensional map, were used to identify the different phases of GaN present. In all samples the texture maps of {113}-type reflections show a very intense reflection pattern with four-fold symmetry, confirming the presence of cubic GaN as the dominant phase. In epilayers grown under non-optimised conditions {1103}-type reflections, forming distorted hexagonal-like patterns, were also observed. Simulations show that these originate from wurtzite-phase inclusions, whose (0001) basal planes are parallel to the

{111} facets of cubic GaN. However, in samples produced under optimised growth conditions the hexagonal patterns were virtually absent with negligible intensities above the background noise level. In these cases the signal originates not from hexagonal inclusions but from *stacking faults* (SFs). Scanning Electron Diffraction TEM studies confirm the absence of hexagonal inclusions in those samples [3]. Faulty stacking of {111} planes in cubic GaN cause a characteristic broadening of selected X-ray reflections normal to the SFs in reciprocal space, which overlaps with the theoretical position of hexagonal wurtzite-type reflections. In conventional reciprocal space maps this diffuse scattering is clearly visible as a weak streak, while hexagonal reflections could not be clearly identified.

1. L. V. Fiorentini, F. Bernardini, F. Della Sala, A. Di Carlo, P. Lugli, *Phys. Rev. B*, 60 (12), (1999), 8849.
2. V.D. Compeán García, I. E Orozco Hinostrroza, A. Escobosa Echavarría, E. López Luna, A. G. Rodríguez, M. A. Vidal, *J. of Crystal Growth*, **418**, (2015), 120.
3. S.-L. Sahonta, M. Frentrup, L.-Y. Lee, M. J. Kappers, R. Oliver, D. Nilsson, J. Shaw, P. Ward, C. Humphreys, D. J. Wallis, *Phase purity analysis of MOVPE-grown cubic GaN epilayers*, International Workshop on Nitride Semiconductors (IWN), (2016).

We thank Innovate UK for the financial support within the Energy Catalyst Round 2 - Early Stage Feasibility scheme (Ref. 132135): "To demonstrate the potential to make low cost, high efficiency LEDs using 3C-SiC substrates".

PA40

INFLUENCE OF THE APPLIED VOLTAGE BIAS ON THE STRAIN FIELD IN A SINGLE GaN NANOWIRE REVEALED BY 3D COHERENT X-RAY DIFFRACTION

S. Lazarev^{1,4}, D. Dzhigaev^{1,2}, Zh. Bi⁵, A. Nowzari⁵, A. V. Zozulya¹, I. Zaluzhnyy^{1,2}, O. Gorobtsov^{1,3}, L. Samuelson⁵, M. Sprung¹ and I. A. Vartanyants^{*1,2}

¹Deutsches Elektronen-Synchrotron DESY, Notkestrasse 85, D-22607 Hamburg, Germany

²National Research Nuclear University MEPhI, Kashirskoye ch. 31, 115409 Moscow, Russia

³NRC Kurchatov Institute, Akademika Kurchatova pl. 1, 123182 Moscow, Russia

⁴National Research Tomsk Polytechnic University (TPU), pr. Lenina 30, 634050 Tomsk, Russia

⁵Lund University, 22100 Lund, Sweden

ivan.vartanyants@desy.de

The wurtzite (hexagonal) structure of GaN nanowires (NWs) is non-centrosymmetric and has an internal electric field along the [0001] direction [1, 2]. Any deformation of the GaN unit cell leads to formation of the internal piezoelectric field and vice versa applied voltage leads to the

strain formation. This effect dramatically influences electron-hole pair recombination and may decrease the efficiency of optoelectronic devices based on GaN NWs. Moreover, the so-called "green gap" problem related to the low efficiency in GaN based green light emitters could be

in touch with piezoelectric and strain fields formation [3]. Therefore, investigation of the influence of the applied voltage on the strain of the NW and the resulting change of the electronic properties of the NW is of significant interest.

In order to study the influence of applied voltage bias on the strain field in a single GaN NW, metal contacts were deposited on two sides on the NW using electron beam lithography. The inner structure of the NW as a function of applied voltage was studied by the coherent x-ray diffraction technique. The experiment was performed at beamline

P10 at synchrotron facility PETRA III (DESY, Hamburg, Germany). During the measurements, the Bragg peak evolution as a function of applied voltage was investigated till electric breakdown of the NW.

1. J. S. Speck, et al., *MRS Bulletin*, **34**, 304-312, (2009). [doi:10.1557/mrs2009.91]
2. F. Boxberg, et al., *Nano Lett.*, **10**, 1108–1112, (2010). [doi:10.1021/nl9040934].
3. F. Scholz, *Semicond. Sci. Technol.* **27**, 024002, (2012). [doi:10.1088/0268-1242/27/2/024002].

PA41

ULTRAFast MELTING OF POLYSTYRENE COLLOIDAL CRYSTALS INVESTIGATED IN PUMP-PROBE EXPERIMENTS AT X-RAY FREE ELECTRON LASER

S. Lazarev^{1,9}, J.-M. Meijer², M. Chollet³, A. Singer⁸, R. P. Kurta⁶, D. Dzhigaev^{1,4}, O. Gorobtsov^{1,5}, G. Williams³, D. Zhu³, Y. Feng³, M. Sikovski³, S. Song³, A. Shabalin¹, N. Mukharamova¹, I. Besedin^{1,4}, I. Zaluzhnyy^{1,4}, E. A. Sulyanova^{1,10}, O. Yefanov⁷, B. Ziaja-Motyka^{7,11}, R. Santra⁷, A. V. Petukhov², and I. A. Vartanyants^{*1,4}

¹Deutsches Elektronen-Synchrotron DESY, Notkestrasse 85, D-22607 Hamburg, Germany

²Debye Institute for Nanomaterials Science, University of Utrecht, Padualaan 8, 3508 TB Utrecht, The Netherlands

³SLAC National Accelerator Laboratory, 2575 Sand Hill Rd, Menlo Park, 94025 CA

⁴National Research Nuclear University MEPhI, Kashirskoye ch. 31, 115409 Moscow, Russia

⁵NRC Kurchatov Institute, Akademika Kurchatova pl. 1, 123182 Moscow, Russia

⁶European XFEL GmbH, Notkestraße 85, D-22607 Hamburg, Germany

⁷Center for Free-Electron Laser Science, DESY, Notkestraße 85, D-22607 Hamburg, Germany

⁸University of California, 9500 Gilman Dr., La Jolla, San Diego, California 92093, USA

⁹National Research Tomsk Polytechnic University (TPU), pr. Lenina 30, 634050 Tomsk, Russia

¹⁰Shubnikov Institute of Crystallography RAS, Leninskii pr. 59, 119333 Moscow, Russia

¹¹Institute of Nuclear Physics, PAS, ul. Radzikowskiego 152, 31-342 Kraków, Poland
ivan.vartanyants@desy.de

Periodic mesoscopic materials have a high potential for a wide variety of applications such as multi-dimensional photonic crystals [1], light manipulation, communication technology, sensors, and future optical computing [2]. The possibility to manipulate the properties of photonic crystals by applying stress, pumping energy, or varying temperature opens new highly potential applications [3,4]. Self-assembled colloidal crystals present a promising bottom-up approach towards the fabrication of photonic materials [5].

The ultrafast melting of polystyrene (PS) colloidal crystals formed by self-assembly of sub-micrometer colloidal spherical particles was studied with picoseconds time resolution in pump-probe experiments at X-ray free electron laser at Linac Coherent Light Source (LCLS) in Stanford, USA at the X-ray pump probe (XPP) beamline. The X-ray Bragg peak parameters, such as integrated intensity, peak position, radial and azimuthal widths were analyzed as a function of time. For these parameters time constant of exponential decay were determined. Our analysis has revealed two time scales in relaxation dynamics of colloidal

crystals. One time is on the order of few tens picoseconds and second, slower on the order of few hundred picoseconds.

Recent theoretical calculations of pumped infrared (IR) laser pulse interaction with a PS colloidal particle reveal full ionization of atoms after the IR pulse and hot electron plasma formation. Therefore, in the experiment plasma crystals in air were formed. The ultrafast dynamics of the plasma crystals will be studied in our future work.

1. W. Martienssen, et al., Springer Handbook of Condensed Matter and Materials Data, **XVIII**, 1121 p. (2005).
2. J. D. Joannopoulos, et al., Princeton University Press, 4th edition, (2008).
3. A.V. Akimov, et al., *Phys. Ref. Letters*, **101**, 033902, (2008).
4. D. M. Beggs, et al., *Phys. Ref. Letters*, **108**, 213901 (2012).
5. D.J. Shaw. Butterworth-Heinemann, 4th edition, ISBN 0-7506-1182-0, (1992).